

LEXNET Low EMF Exposure Future Networks

D3.2 release 2 Appendices

Contractual delivery date: M16
Actual delivery date: M24

Document Information

Version	V2.0	Dissemination level	PU							
Editor	S. BORIES (CEA-L	S. BORIES (CEA-LETI)								
Other authors	,	T), M. LE HENAFF (SAT), Y. ANDEZ (TTI), A. SANCHEZ								

PROPRIETARY RIGHTS STATEMENT

This document contains information, which is proprietary to the LEXNET Consortium. Neither this document nor the information contained herein shall be used, duplicated or communicated by any means to any third party, in whole or in parts, except with prior written consent of the LEXNET consortium.



2

	DASSONVILLE (CEA), S. BORIES (CEA), T. SARREBOURSE (ORANGE) M. KOPRIVICA (TKS), A. NEŠKOVIĆ (TKS), M. POPOVIĆ (TKS), J. MILINKOVIĆ (TKS), S. NIKŠIĆ (TKS), M. MACKOWIAK, L. CORREIA (INOV), C. ROBLIN (TPT), A. SIBILLE (TPT), R. HASHMAT (TPT)
Abstract	This document corresponds to the appendices associated to the deliverable D3.2 release 2
Key words	Dosimeter, wideband, wearable, correction factor, uncertainty.

Project Information

Grant Agreement n°	318273
Dates	1 st November 2012 – 31th October 2015

Document approval

Name	Position in project	Organisation	Date	Visa
Joe Wiart	Coordinator	Orange	13/01/2015	OK

Document history

Version	Date	Modifications	Authors
V1.0	10/04/2014	revised version from review	S. Bories
V2.0	18/12/2014	Second release, appendices only	S. Bories

Version: V2.0



Table of contents

APPENDIX 2: CHARACTERIZATION OF THE TRAFFIC IMPACT OF EMF	
MEASUREMENTS	6
Long-term variability of EMF strength - Paris measurements	6
Long-term variability of electromagnetic field strength - Belgrade measurements	8
Uncertainty caused by telecommunication traffic and transmitter functionalities	15
APPENDIX 3: GUIDELINES ON THE EXPRESSION OF UNCERTAINTY IN LEXNET	
DOSIMETER MEASUREMENTS	21
Uncertainity caused by Measurement device - u(Md)	
Uncertainty of the calibration of the sensor - u(MS)	
Uncertainty of the Calibration of the Sensor - u(MS)	
Uncertainty of the anisotropy - u(A)	
Uncertainty caused by the usage of monoaxial probe - u(MA)	
Uncertainty caused by mismatching - u(VSWR)	
Uncertainty caused by "electrical noise" - u(Noise)	
Uncertainty caused by drift in the transmitting powers, measurement equipment, temperature and	23
humidity - u(Drift)	23
Uncertainty caused by human bodies - u(Body)	
Uncertainty caused by small-scale fading - u(Fad)	
Uncertainty caused by telecommunication traffic and transmitter functionalities - u(Traff)	
Total (combined) standard uncertainty	
Expanded uncertainty	
,,,,,,,,,,,,,,,,,,,,,,,,,,,,,,,,,,,,,,,	
APPENDIX 4: PRESENTATION OF THE CHANNEL MODEL USED IN SECTION 4	28
APPENDIX 5: DETAILS AND MEASUREMENTS OF THE EXTRAPOLATION FROM	
MONOAXIAL TO ISOTROPIC FIELD PROBE STUDY	31
APPENDIX 6: SPECTRUM RESULTS FOR THE DOSIMETER STUDY IN REAL ENVIRONMENT	35
LIVIIIOIVILLIVI	
APPENDIX 7: STUDY OF OPTIMUM EMF MEASUREMENT METHODOLOGY FOR	
EXPOSURE EVALUATION	38



List of Acronyms

The acronyms can be found in the main D3.2 r2 document.

List of figures

Figure 1: Frequency selective measurement system	6
Figure 2 Example of the variation of the surface power density over 24 hours for the DCS	7
Figure 3 Variability of the surface power density over 24h for GSM 900	
Figure 4 Variability of the surface power density over 24h for DCS	8
Figure 5 Variability of the surface power density over 24h for UMTS 2100	8
Figure 6 Time variability of electric field strength for GSM	11
Figure 7 Probability density function of electric field strength for "all days" - GSM	11
Figure 8 Probability density function of electric field strength for "working days" - GSM	12
Figure 9 Time variability of electric field strength for DCS	12
Figure 10 Probability density function of electric field strength for "all days" - DCS	13
Figure 11 Probability density function of electric field strength for "working days" - DCS	13
Figure 12 Time variability of electric field strength for UMTS	14
Figure 13 Probability density function of electric field strength for "all days" - UMTS	
Figure 14 Probability density function of electric field strength for "working days" - UMTS	
Figure 15: Traffic uncertainty with regards to time averaging intervals for "all days" - GSM	
Figure 16: Traffic uncertainty with regards to time averaging intervals for "working days" - GSM	17
Figure 17 Traffic uncertainty with regards to time averaging intervals for "all days" - DCS	
Figure 18 Traffic uncertainty with regards to time averaging intervals for "working days" - DCS	
Figure 19 Traffic uncertainty with regards to time averaging intervals for "all days" - UMTS	
Figure 20 Traffic uncertainty with regards to time averaging intervals for "working days" – UMTS	
Figure 21 Electric field strength (mV/m) with regards to time for scenario 1	
Figure 22 Extrapolation factors with regards to time for scenario 1	
Figure 23 Probability density function for extrapolation factor n for scenario 1	
Figure 24: Spectrum analyser results GSM-DL at the three locations described in Table 41	
Figure 106 of D3.2	35
Figure 25: Spectrum analyser results DCS-DL at the three locations described in Table 41	
Figure 106 of D3.2	
Figure 26: Spectrum analyser results UMTS-DL at the three locations described in Table 41	
Figure 106 of D3.2	37
Figure 28: Time domain based EMF measurement platform (a) measurement setup,	(a)
measurement technique.	
Figure 29: Locations for the measurements with the time domain based platform	
Figure 30: Measurement results for GSM-DL with different post-processing techniques	
1m10 probe height at two locations	41
two locationstwo locations	
Figure 32: Measurement results for DCS-DL with different post-processing techniques at	43
two locationstwo locations	
two locations. Figure 33: Measurement results for UMTS-DL with different post-processing techniques at	44 • th •
two locations	
Figure 34: Measurement results for LTE VII-DL with different post-processing techniques at	
two locations	
two iooutions	→ /

Version: V2.0



List of Tables

Table 1 Measured frequency bands		
Table 3 Traffic uncertainty (%) with regards to time averaging intervals for DCS		
Table 4 Traffic uncertainty (%) with regards to time averaging intervals for UMTS	Table 2 Traffic uncertainty (%) with regards to time averaging intervals for GSM	. 16
Table 5 Traffic uncertainty (%) with regards to averaging intervals for GSM, DCS and UMTS		
Table 6 : Parameters WINNER2/WINNER+ channel models for ten environments		
Table 7: Mean values, medians, standard deviations and uncertainties of extrapolation factors		
Table 8 Comparison of mean values, medians, standard deviations and uncertainties for n for all scenarios		
Scenarios		
Table 9: Measurement setup for each signal type		
Table 10: Comparison of different techniques for EMF exposure calculation for the GSM-DL signal at location#1		
location#2	Table 10: Comparison of different techniques for EMF exposure calculation for the GSM-DL signal	al at
Table 12: Comparison of different techniques for optimum EMF exposure for the DCS-DL signal at location#1	· · · · · · · · · · · · · · · · · · ·	
location#1		
Table 13: Comparison of different techniques for optimum EMF exposure for the DCS-DL signal at location#2	· · · · · · · · · · · · · · · · · · ·	
location#1	Table 13: Comparison of different techniques for optimum EMF exposure for the DCS-DL signal ocation#2	al at
Table 15: Comparison of different techniques for optimum EMF exposure for the UMTS-DL signal at location#2	· · · · · · · · · · · · · · · · · · ·	
Table 16: Comparison of different techniques for optimum EMF exposure for the LTEVII-DL signal at location#1	Fable 15: Comparison of different techniques for optimum EMF exposure for the UMTS-DL signal ocation#2	al at 45
location#2	Fable 16: Comparison of different techniques for optimum EMF exposure for the LTEVII-DL signal	al at
Table 18: Proposed measurement techniques for the different telecommunication standards in the		
	Table 18: Proposed measurement techniques for the different telecommunication standards in	the

Version: V2.0 5



APPENDIX 2: CHARACTERIZATION OF THE TRAFFIC IMPACT OF EMF MEASUREMENTS

Long-term variability of EMF strength - Paris measurements

A measurement campaign has been done with the aim to collect data about exposure level due to the mobile network Down-Link traffic in an indoor environment. The measurement campaign has been done in different environments as urban and rural areas. Information about the variability of the electromagnetic field can be extracted from this campaign.

The measurement system used for this campaign consisted of:

- 3-axis probe (SATIMO),
- a spectrum analyzer Agilent MXA 9020,
- a software (Xplora developed by Orange Labs) included in the analyzer which drives the measurements and saves the E field (E) values in V/m.

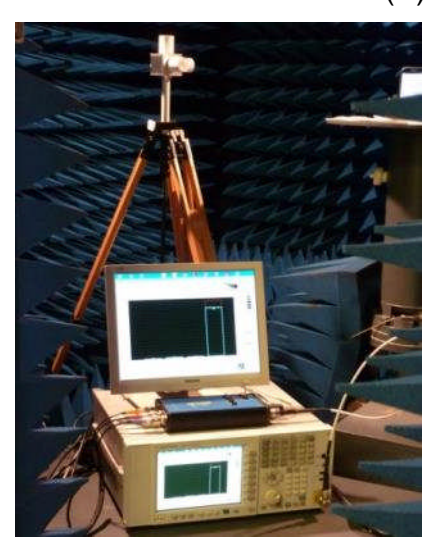


Figure 1: Frequency selective measurement system

The measured bands were selected in accordance with table 1.

Table 1 Measured frequency bands

Band	Center frequency (MHz)	Span (MHz)
GSM 900 DL	945	40
DCS DL	1840	80
UMTS DL	2150	80

Twenty measurements were done in 9 different sites in urban zone and 6 measurements in 3 different sites in rural zone in Paris and around. For each site,

Version: V2.0



and when it was possible, the system was installed at different places (bedroom, kitchen, and lounge) but was not moved during 24 hours.

The sampling rate was chosen in such a way to have a measurement of each band every 10 seconds during 24 hours.

In figure 2 is given an example of the signal obtained from the 24 hours measurements for the DCS in an urban configuration. The amplitude corresponds to the surface power density S in W/m^2 where $S = E^2/377$.

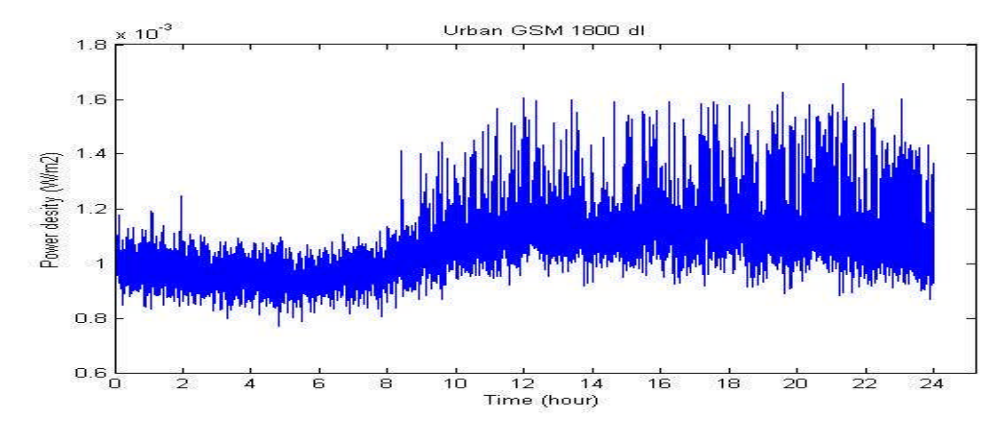


Figure 2 Example of the variation of the surface power density over 24 hours for the DCS

For each frequency band all the measurements have been normalized to their average value over 24 hour. A moving average and the standard deviation have been calculated for the signal at each hour.

In figures 119-118, the results for GSM 900, DCS, and UMTS are given, respectively.

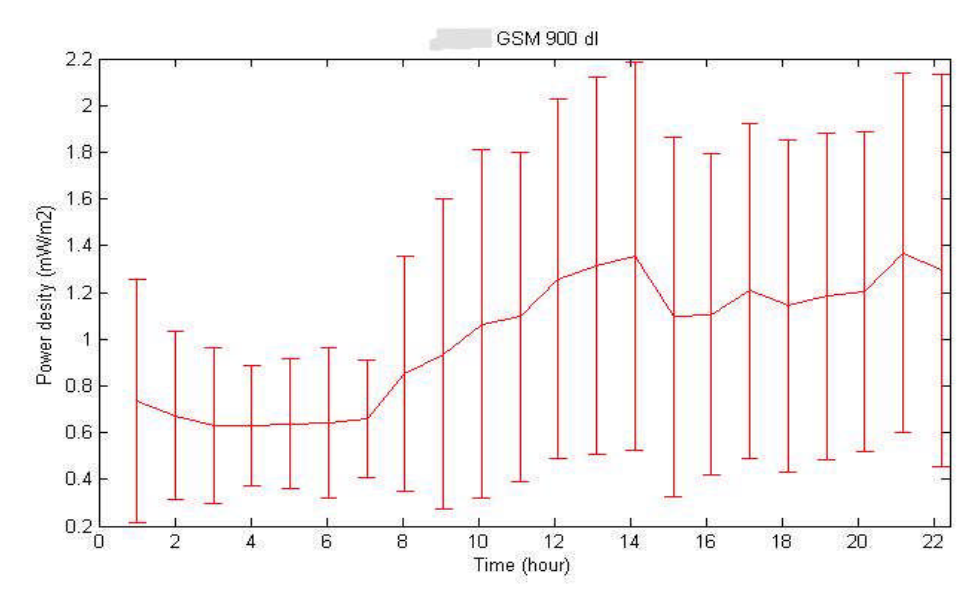


Figure 3 Variability of the surface power density over 24h for GSM 900

Version: V2.0



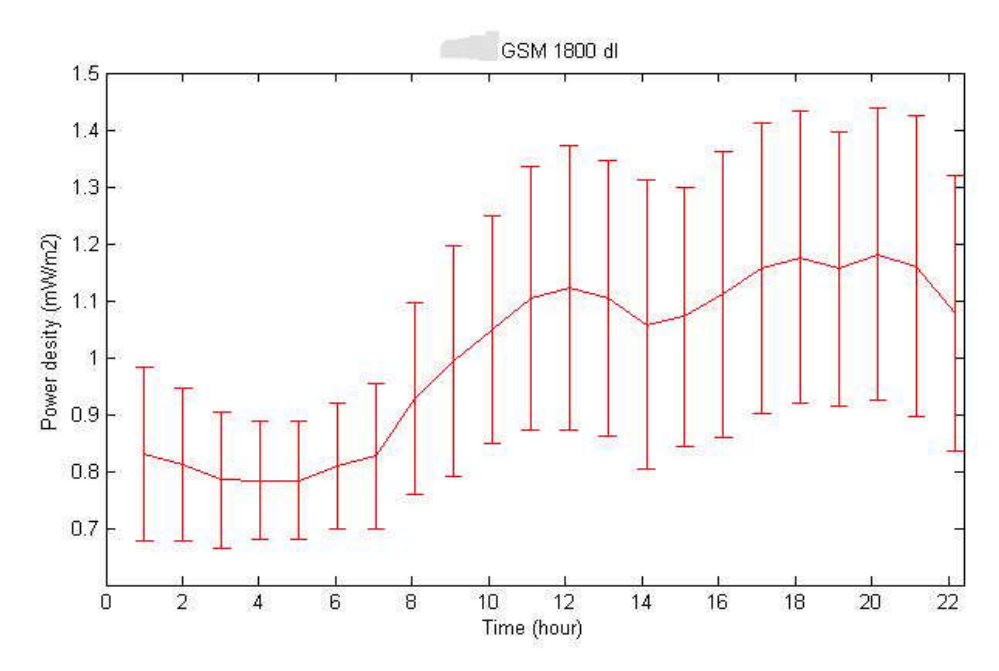


Figure 4 Variability of the surface power density over 24h for DCS

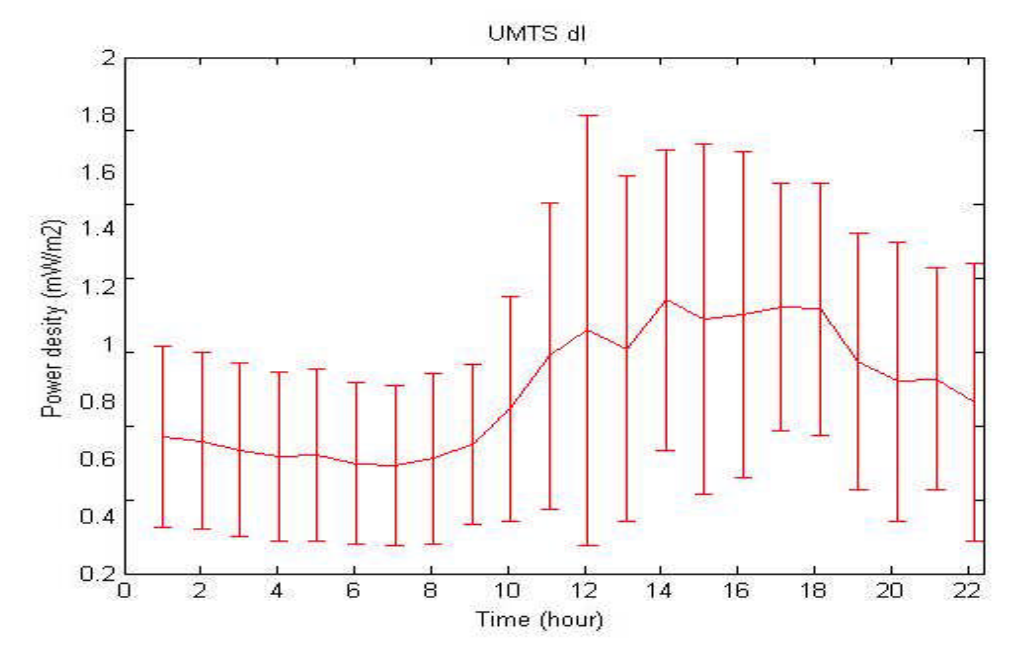


Figure 5 Variability of the surface power density over 24h for UMTS 2100

Long-term variability of electromagnetic field strength - Belgrade measurements

For the analysis which is the subject of the study, the calibrated Rohde&Schwarz portable EMF measurement system was used. Spectrum analyzer Rohde&Schwarz FSH6 and measuring antenna Rohde&Schwarz TS-EMF, in the form of an isotropic radiator, are the main measuring components of the system. This system is designed

Version: V2.0



for frequency selective measurement of electric field strength in the frequency range from 30 MHz to 3 GHz. System is controlled with the softer module White Tigress Baby - Measurements, specially developed for the long-term measurements in Radio-communications Laboratory, School of Electrical Engineering, University of Belgrade for the purpose of LEXNET project.

Measurements were conducted with the sampling interval of 9.5 seconds and RMS detector was used. Following parameters were used for the measurements:

- Center frequency 947.5MHz and Channel bandwidth 25MHz (GSM band)
- Center frequency 2140MHz and Channel bandwidth 60MHz (DCS band) and
- Center frequency 1830.1MHz and Channel bandwidth 50.2MHz (UMTS band).

Intensive measurements of electromagnetic field strength in Belgrade were carried out at 3 different locations in urban area of Belgrade. Two locations were chosen as measurement locations in indoor environment and one in outdoor. Measurements were performed in time intervals of 7 days for each location. During the 7-day measurements the system was stationary with an antenna mounted on a tripod. In such a way measurement results for GSM, DCS and UMTS DL bands were obtained.

The examples of measurement results for one test location are shown in Figures 6-14. Specifically, figures 6, 9 and 12 represent electric field strength time variability for GSM, DCS and UMTS, respectively. Despite the fact that the measurement results are shown for only one test location, discussions and conclusions are based on results obtained for all three locations.

Time variability of electric field strength for all three systems clearly shows that for each day two different periods can be observed - one with high levels and one with low levels. Electric field strength for all three systems has very similar daily behaviour. At the beginning of the day (midnight), the strength of electric field decreases. After that there is a period approximately from 2:00 to 7:00 in which electric field strength has the lowest level. Beginning with the morning, the electric field strength starts to increase until approximately 9:00 when it reaches the level of the active part of a day. The active part of the day has the highest values of electric field strength and lasts until approximately 23:00. At the very end of the day, electric field strength starts to decrease. In accordance with the observed behaviour of electric field strength the day was separated in two distinctive periods: "active hours" (9h-23h) and "night hours" (23h-9h).

Measurement results show that the short-term variability during the "active hours" is higher than during the "night hours". On the other hand, when average value of this variability is considered, it is opposite case. Average values are fairly stable during the all period of "active hours" and have the highest levels. Some exceptions are detected for UMTS, where the distinctive periods with a significant increase of electric field strength during the "active hours" are observed.

As already stated, during the "night hours" the short-term variability of the electric field strength is lower than during the "active hours". As opposite to "active hours" the average values have significant changes for "night hours". At the beginning of "night hours" significant decrease of average values can be detected. Also, at the end of the Version: V2.0



"night hours" significant increase of average values can be obtained. On the other hand, period in middle of the "night hours" (approximately from 2:00 to 7:00) is time of inactivity in which the short-term variability, as well as average values of the electric field strength, have their lowest values.

Regarding the days of the week, it can be concluded that the weekend days are slightly different from the working days. These differences are manifested in the smaller differences between average values of the electric field strength of the "active hours" and "night hours" during the weekend, than for the working days.

For more detailed analysis two specific categories for 7-day week were distinguished: "working days" (Monday to Friday) and "all days" (Monday to Sunday). Also, the day was divided in two distinctive periods: "active hours" (9h-23h) and "night hours" (23h-9h). According to this, 6 different categories were analysed:

- "all days all hours",
- "working days all hours",
- "all days active hours",
- "working days active hours",
- "all days night hours" and
- "working days night hours".

Probability density function of the electric field strength for the previously defined 6 categories is presented on figures 119 and 121 for GSM, figures 122 and 124 for DCS, and figures 125 and 127 for UMTS.

In the case of GSM and DCS, probability density functions for "all hours" have behaviour which is similar to normal distribution (for "all days" category as well as for "working days" category). On the other hand, probability density function for UMTS has a behavior similar to log-normal distribution for "all days" category as well as for "working days" category.

Considering probability density functions for "active hours" and "night hours" separately, it can be concluded that both types of distributions have a similar behaviour than the "all hours" distributions, with the only difference in average values. The distributions for GSM and DCS have behavior similar to normal distribution, while the UMTS distribution behavior is again similar to log-normal distribution.

Version: V2.0 10



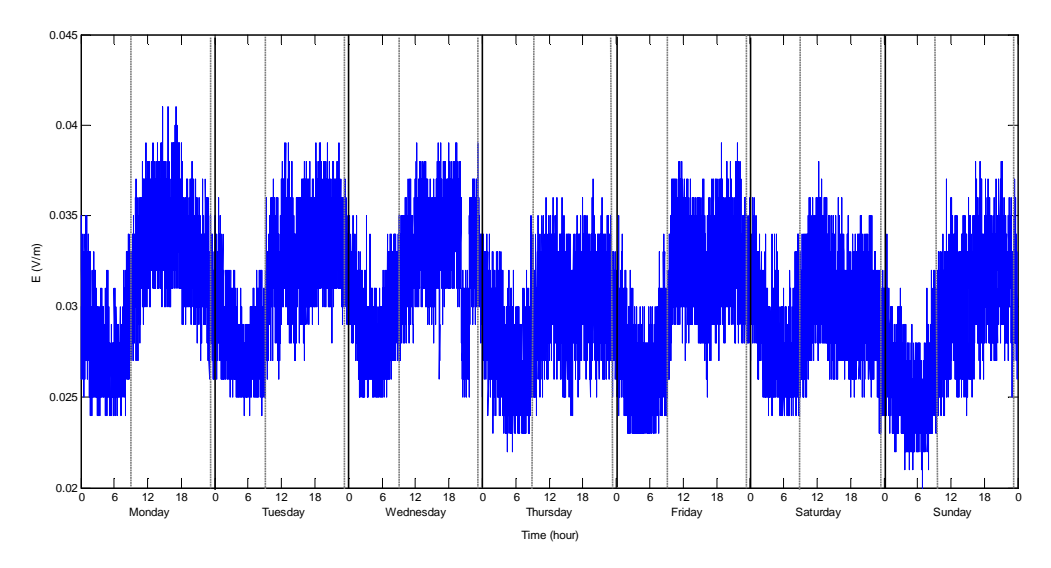


Figure 6 Time variability of electric field strength for GSM

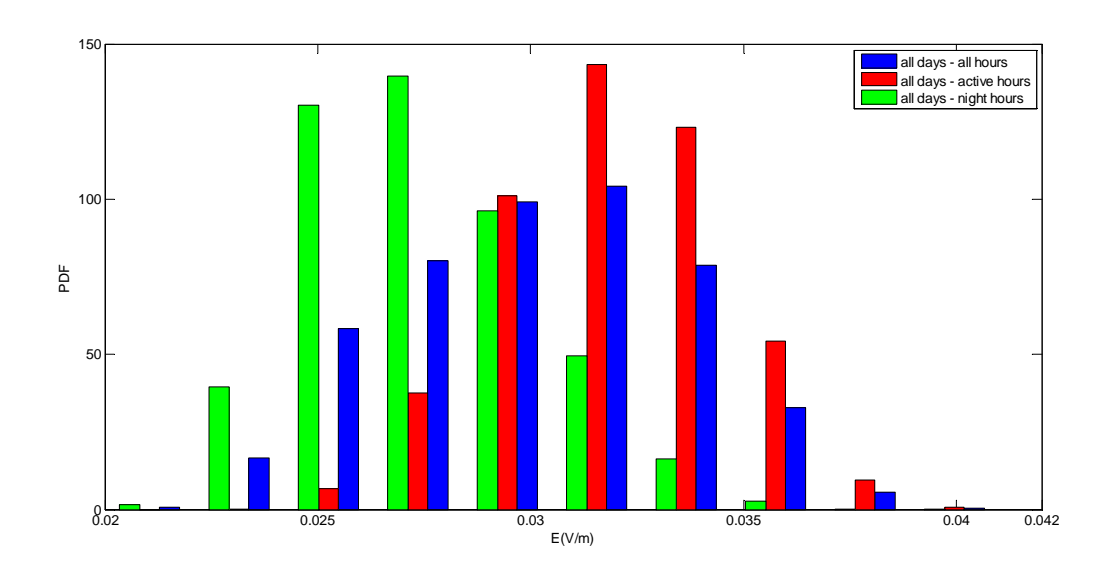


Figure 7 Probability density function of electric field strength for "all days" - GSM



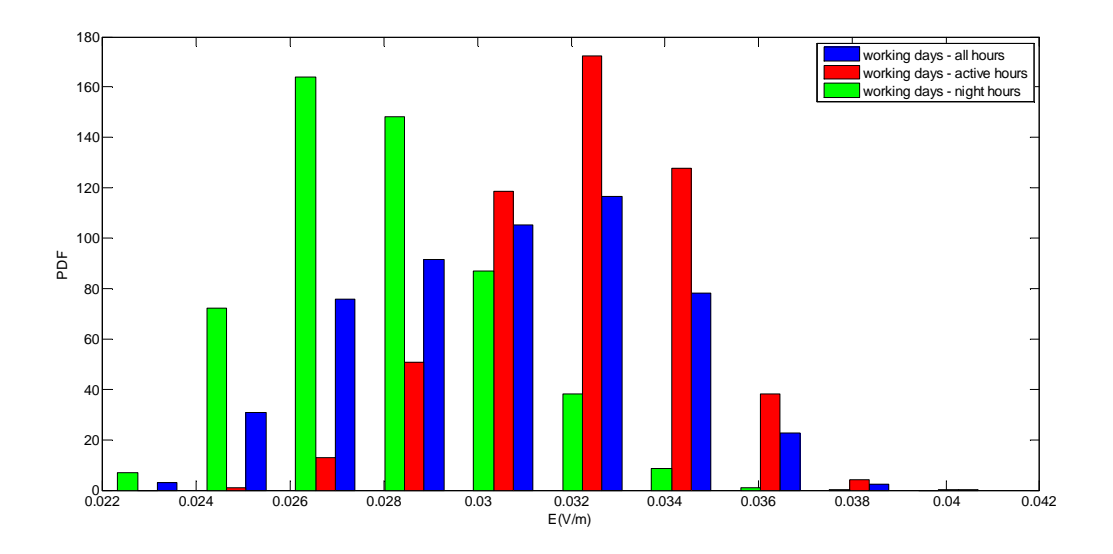


Figure 8 Probability density function of electric field strength for "working days" - GSM

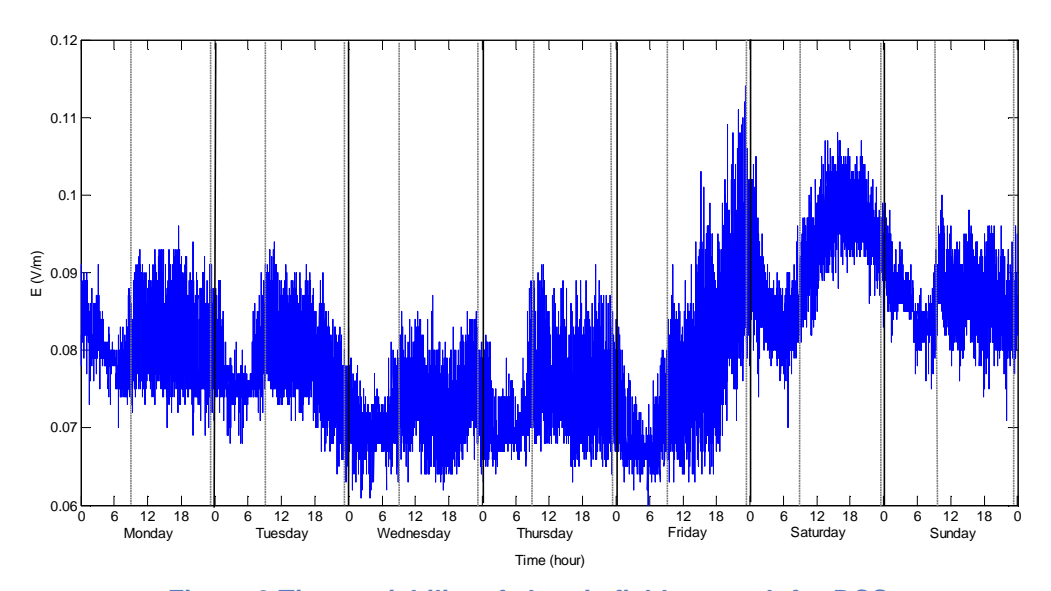


Figure 9 Time variability of electric field strength for DCS



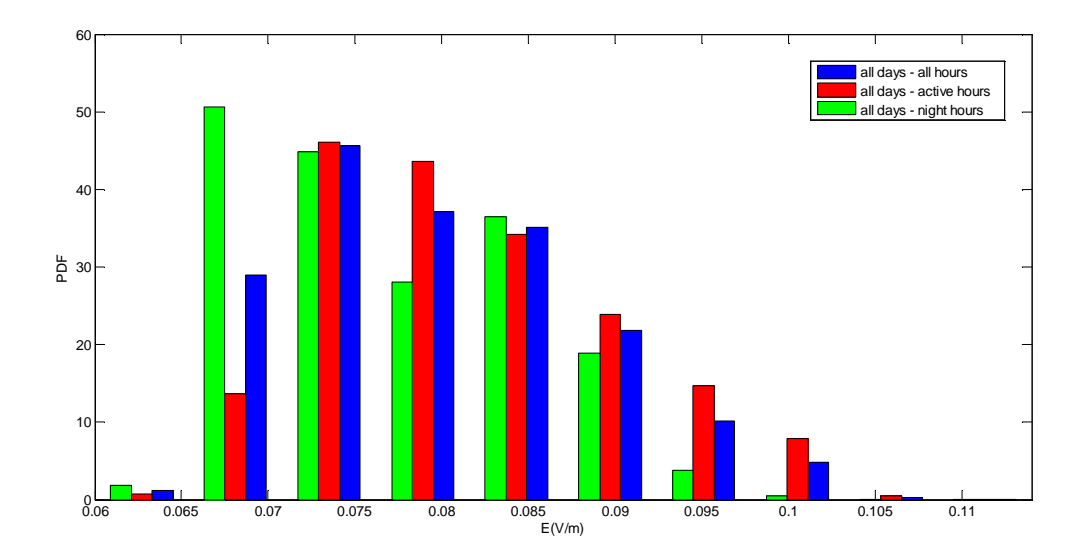


Figure 10 Probability density function of electric field strength for "all days" - DCS

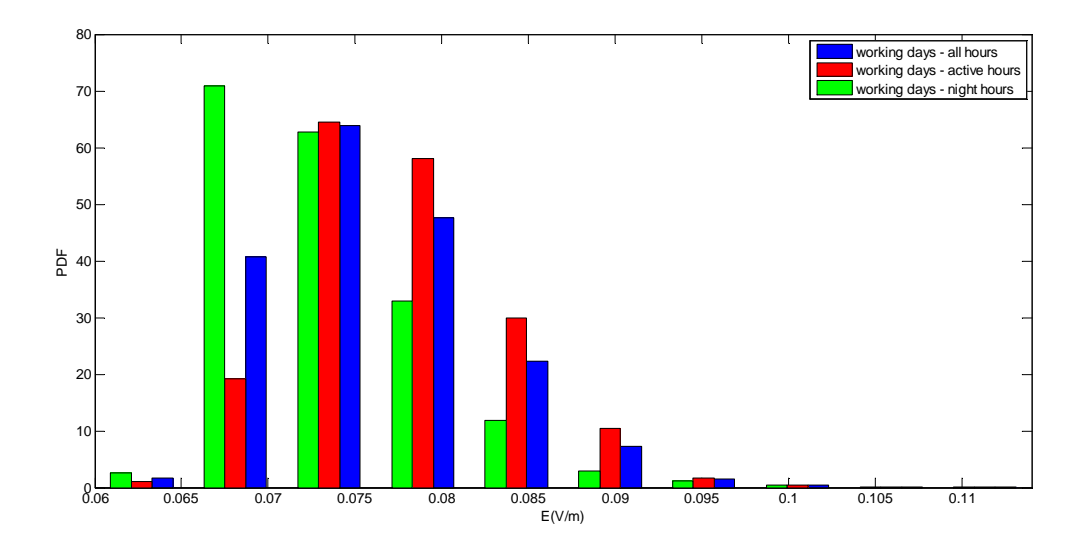


Figure 11 Probability density function of electric field strength for "working days" - DCS



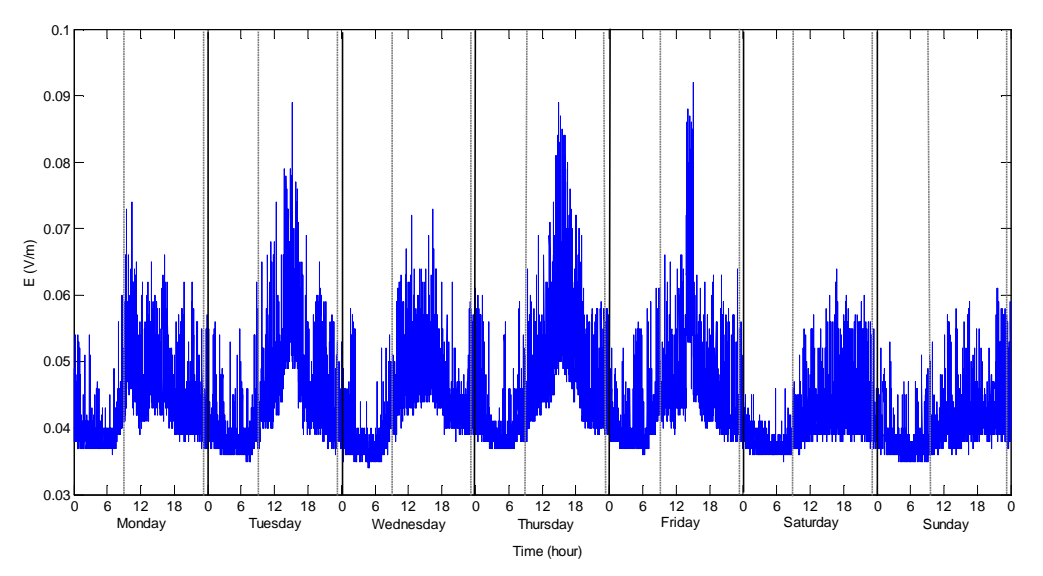


Figure 12 Time variability of electric field strength for UMTS

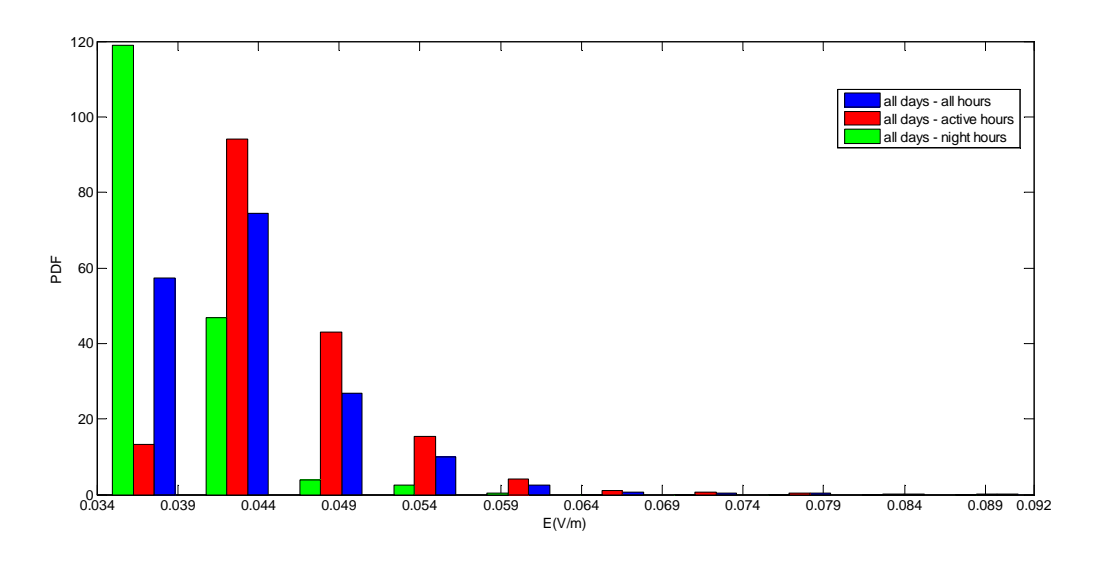


Figure 13 Probability density function of electric field strength for "all days" - UMTS



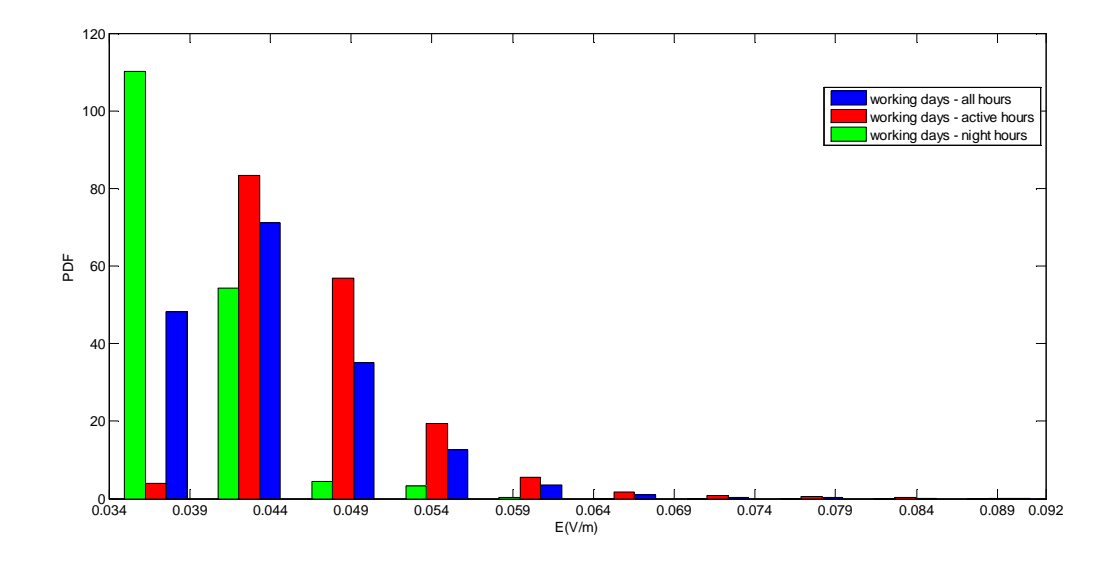


Figure 14 Probability density function of electric field strength for "working days" - UMTS

Uncertainty caused by telecommunication traffic and transmitter functionalities

With regards to the previously analyzed effects which lead to greater instability of the DL electromagnetic field strength, an additional uncertainty caused by telecommunications traffic and transmitter functionalities must be taken into account.

For each of previously defined categories, the uncertainty caused by telecommunications traffic and transmitter functionalities is analyzed for different time intervals of averaging: 10s, 30s, 1min, 6min, 15min, 30min, 1h, 3h, 6h and 10h. For the purpose of averaging, the total data set was divided in non-overlapping intervals of the defined duration. For each interval, a unique average value was determined with the exception of the intervals of 10s where no averaging were done. The maximum value of the averaging interval was 10h and it was determined according to the duration of "night hours".

The uncertainty caused by telecommunications traffic and transmitter functionalities can be determined by statistical analysis of a series of average values [28] and [29]. In the first step, the mean value E_{meas} and the standard deviation $\sigma(E_{meas})$ are determined using:

$$E_{meas} = \frac{1}{N} \sum_{i=1}^{N} E_{meas i} \tag{1}$$

$$\sigma(E_{meas}) = \sqrt{\frac{1}{N-1} \sum_{i=1}^{N} (E_{meas i} - E_{meas})^2}$$
 (2)



where $E_{meas\,i}$ denotes *i*-th averaged value and N is the total number of averaged values.

The relative ratio of the standard deviation and the mean value defines the traffic uncertainty *u(Traff)*:

$$u(Traff) := \frac{\sigma(E_{meas})}{E_{meas}} \tag{3}$$

Using the three previous equations, the traffic uncertainties for all 6 categories defined in previous section are determined.

Results of the uncertainty caused by telecommunication traffic and transmitter functionalities with regards to averaging interval, averaged over all 3 test locations are presented in tables 49 to 51, and 4 for GSM, DCS and UMTS, respectively. Also, in these tables, the values of the uncertainties averaged over all 3 test locations are given. The obtained results are also presented graphically in Figure 15 and Figure 16.

Table 2 Traffic uncertainty (%) with regards to time averaging intervals for GSM

Category				Α	veraging	interval								
Category	10s	30s	1min	6min	15min	30min	1h	3h	6h	10h				
"all days – all hours"	10.24	9.38	9.10	8.69	8.55	8.44	8.34	7.92	7.05	6.59				
"working days - all hours"	10.48	9.59	9.30	8.87	8.75	8.65	8.53	8.14	7.17	6.75				
"all days – active hours"	8.34	7.21	6.84	6.29	6.08	5.91	5.74	5.31	5.04	4.29				
"working days – active hours"	8.55	7.00	6.61	6.02	5.80	5.62	5.46	4.88	4.59	4.08				
"all days - night hours"	9.06	8.24	7.97	7.58	7.47	7.38	7.30	6.95	6.47	4.76				
"working days - night hours"	9.04	8.18	7.89	7.48	7.36	7.28	7.17	6.84	5.07	4.31				

Table 3 Traffic uncertainty (%) with regards to time averaging intervals for DCS

Category		Averaging interval								
Category	10s	30s	1min	6min	15min	30min	1h	3h	6h	10h
"all days – all hours"	7.99	7.59	7.46	7.27	7.18	7.10	7.01	6.56	6.07	5.54
"working days - all hours"	7.47	7.04	6.90	6.70	6.55	6.46	6.36	5.80	5.22	4.51
"all days – active hours"	8.65	8.19	8.04	7.82	7.73	7.63	7.49	7.29	6.63	5.77
"working days - active hours"	8.23	7.70	7.53	7.25	7.12	6.99	6.83	6.43	5.61	4.63
"all days - night hours"	6.26	5.90	5.79	5.65	5.60	5.59	5.51	5.56	5.42	5.50
"working days - night hours"	4.92	4.53	4.40	4.24	4.17	4.15	4.02	4.02	3.82	3.85

Version: V2.0 16



Table 4 Traffic uncertainty (%) with regards to time averaging intervals for UMTS

Category				-	Averagin	j interval									
Category	10s	30s	1min	6min	15min	30min	1h	3h	6h	10h					
"all days – all hours"	14.35	13.18	12.76	12.12	11.91	11.73	11.54	11.02	10.07	9.13					
"working days - all hours"	14.29	13.05	12.60	11.92	11.72	11.50	11.32	10.72	9.77	8.64					
"all days – active hours"	13.37	11.84	11.29	10.41	10.09	9.81	9.53	9.05	7.96	5.64					
"working days - active hours"	13.04	11.44	10.84	9.89	9.55	9.25	8.90	7.68	6.12	4.57					
"all days - night hours"	11.15	10.09	9.70	9.15	8.96	8.82	8.70	8.17	5.59	3.46					
"working days - night hours"	11.50	10.38	9.96	9.35	9.16	9.02	8.89	8.37	5.59	3.32					

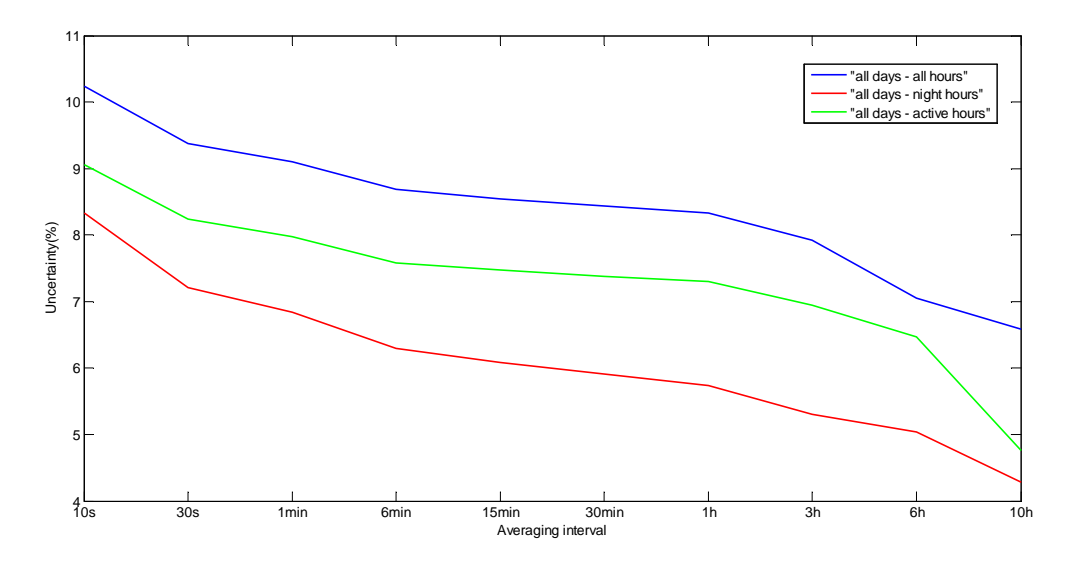


Figure 15: Traffic uncertainty with regards to time averaging intervals for "all days" - GSM

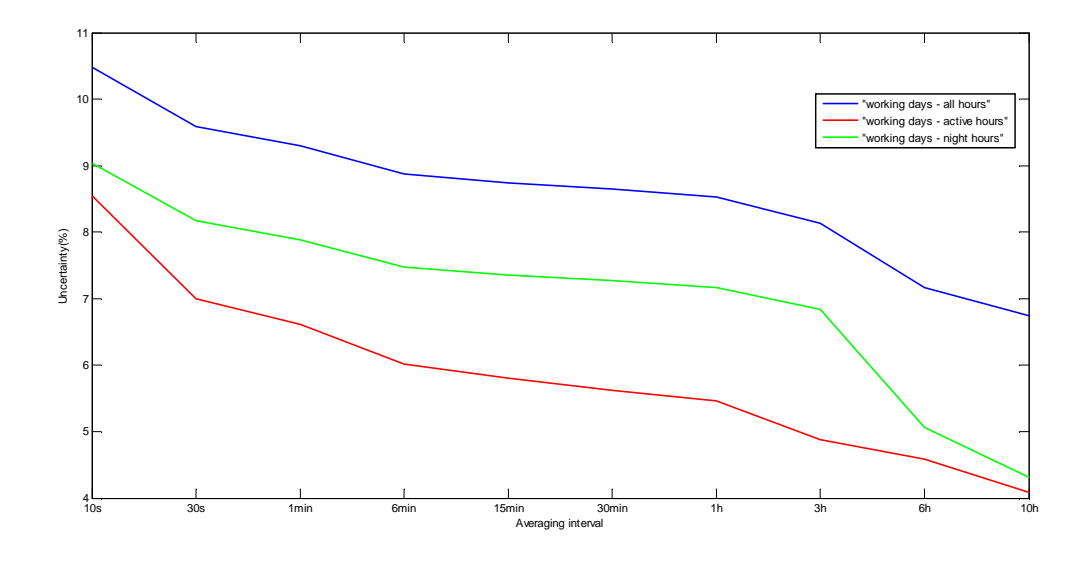


Figure 16: Traffic uncertainty with regards to time averaging intervals for "working days" -



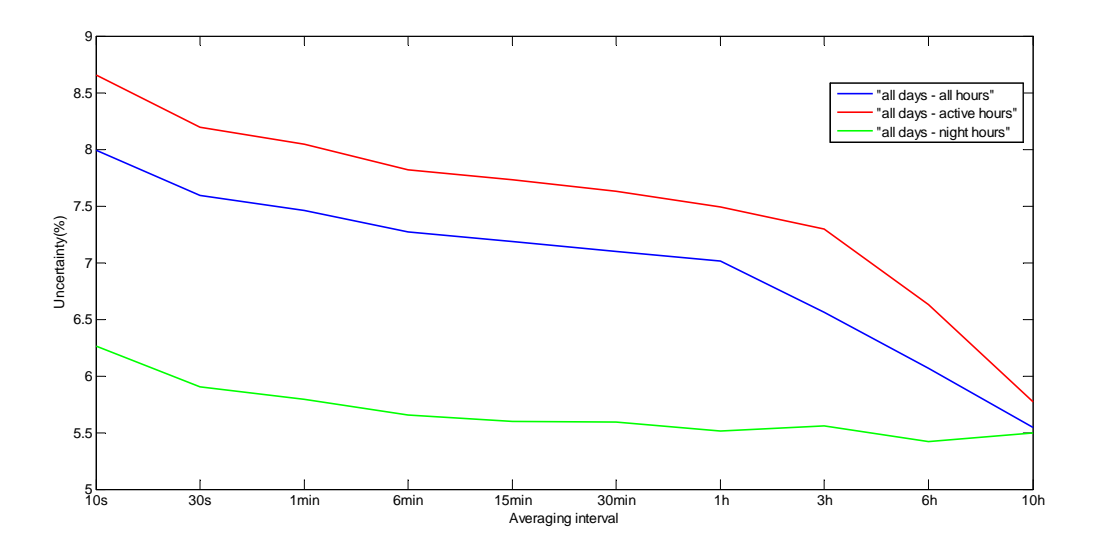


Figure 17 Traffic uncertainty with regards to time averaging intervals for "all days" - DCS

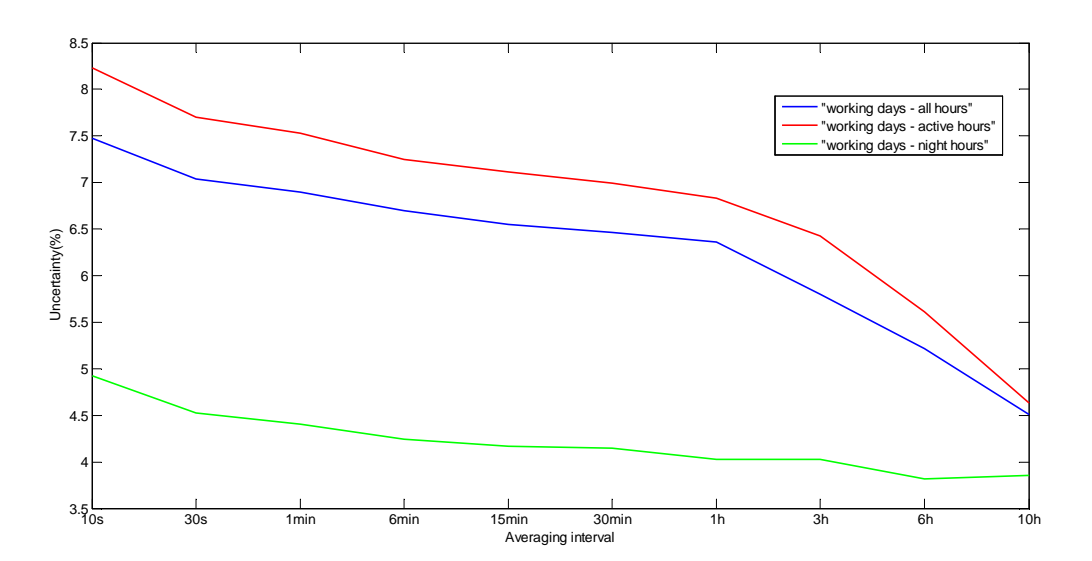


Figure 18 Traffic uncertainty with regards to time averaging intervals for "working days" - DCS



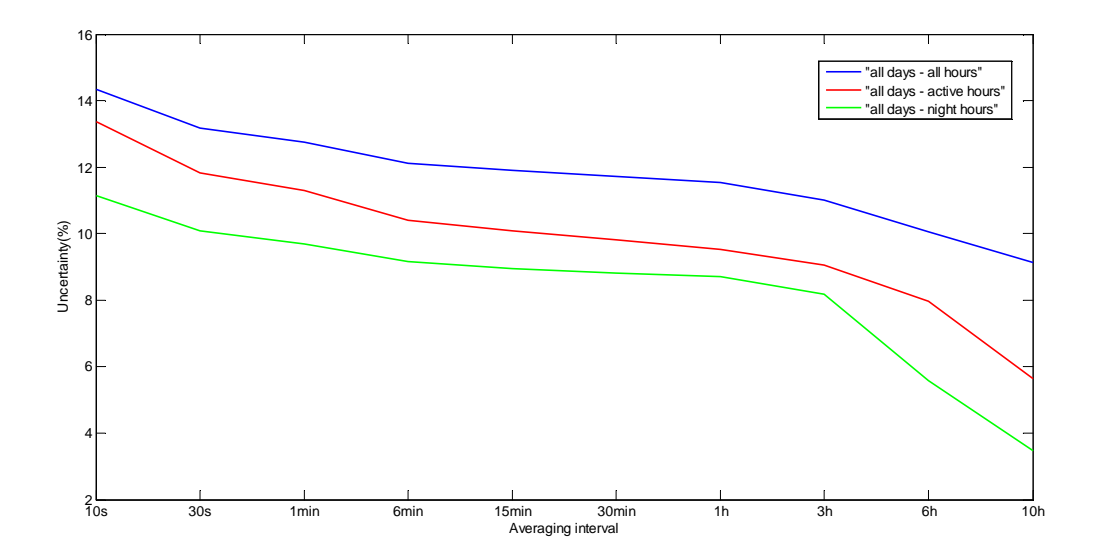


Figure 19 Traffic uncertainty with regards to time averaging intervals for "all days" - UMTS

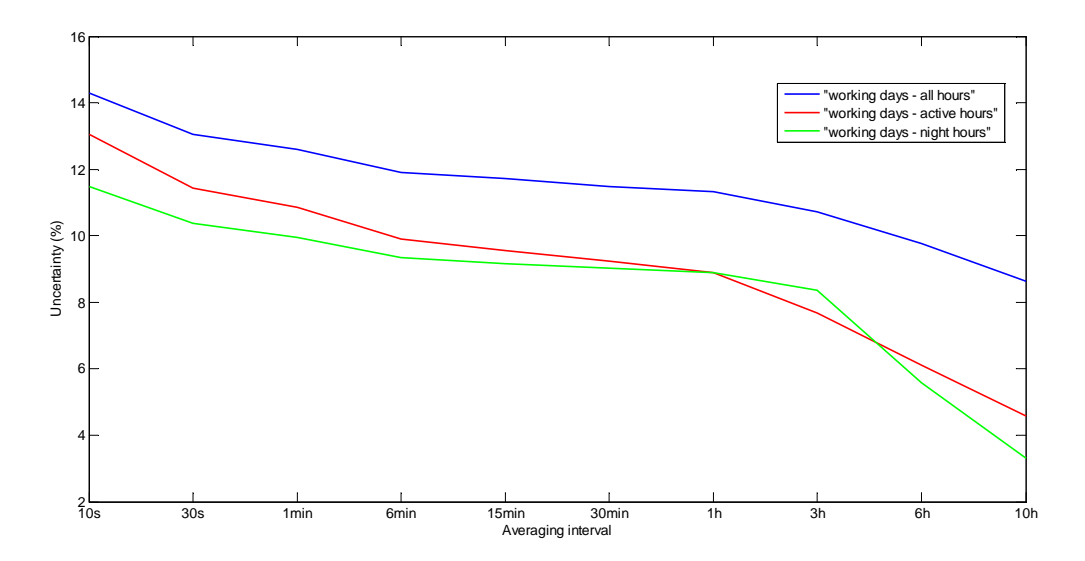


Figure 20 Traffic uncertainty with regards to time averaging intervals for "working days" – UMTS

In addition, the uncertainty caused by telecommunications traffic and transmitter functionalities is analyzed for averaging intervals of all hours (24 hours), active hours (14 hours) and night hours (10 hours). Results averaged over all 7 test locations are presented in Table 5. These results show that measurement uncertainty for values averaged over all hours (all day), active hours and night hours are below 5%.

Version: V2.0



Table 5 Traffic uncertainty (%) with regards to averaging intervals for GSM, DCS and UMTS

System	Category	Averaging interval					
	Calegory	Night hours	Active hours	All hours			
CCM	"all days"	4.08	4.72	3.83			
GSM	"working days"	4.04	4.31	3.57			
DCS	"all days"	4.05	4.79	3.86			
	"working days"	4.18	4.40	3.67			
UMTS	"all days"	3.76	4.67	3.68			
	"working days"	4.00	4.30	3.51			



APPENDIX 3: GUIDELINES ON THE EXPRESSION OF UNCERTAINTY IN LEXNET DOSIMETER MEASUREMENTS

These guidelines provide general rules for evaluating and expressing uncertainty in measurements carried out by LEXNET dosimeter. According to [26], when reporting the result of a measurement of a physical quantity, it is obligatory that some quantitative indication of the quality of the result be given so that those who use it can assess its reliability. Without such an indication, measurement results cannot be compared, either among themselves or with reference values given in a specification or standard. Uncertainty of measurement is parameter, associated with the result of a measurement, that characterizes the dispersion of the values that could reasonably be attributed to the measurand.

Evaluation of uncertainty in measurements carried out by LEXNET Exposure Index (EI) dosimeter is based on the [26, 27, 28, 29, 30]. In order to estimate the uncertainty of measurement, it is generally necessary to know the "model" of the measuring system. In the considered case, the measurements are performed by an integrated system that directly shows the measured values. However, these measurements are considered "indirect". In this case the estimation of measurement uncertainty is carried out mainly on the basis of parameters that can be found in the technical specifications and certificates of calibration of the measuring system, based on the associated standard uncertainties.

In the following text, the assessment of the impact of significant parameters that contribute to the measurement uncertainty is discussed.

Uncertainity caused by Measurement device - u(Md)

Within the considered integrated measurement system (LEXNET Exposure Index dosimeter), as a measuring device a specific spectrum analyzer is used. The uncertainty caused by spectrum analyzer can be determined in two ways:

- based on the technical specifications of the manufacturer (provided that the relevant features of the analyzer are within the limits of the specified accuracy, which is evidenced by a certificate of calibration), or
- based on data from the calibration certificate for the individual parts (subsystems) of the device and based on the technical specifications of the manufacturer's knowledge of the "model" of the measuring device.

Using the second approach lower values of uncertainty are usually obtained, which provides the measurements of greater accuracy.

However, within this project the first approach will be applied. According to the manufacturer's specifications, probability density function for this type of uncertainty is rectangular.

Version: V2.0



Uncertainty of the calibration of the sensor - u(MS)

In the calibration phase, the sensor is immersed in a uniform electric field of a known constant intensity. Calibration process is obviously associated with an uncertainty depending strictly on the calibration chain: power meters, antennas, anechoic chamber, TEM cells, etc. These levels of uncertainty are the "best measurement capability" of the laboratory and they can vary depending on the calibration level and frequency. Calibration laboratories report this uncertainty values into Calibration Certificate. The probability distribution function for this type of uncertainty is considered to be Gaussian.

Uncertainty of the Antenna Factor Interpolation - u(FA)

During the calibration process, the antenna factors are determined for discrete operating frequencies. For frequencies that do not correspond to the frequencies for which the antenna factors are determined the interpolation should be done. However, interpolation process brings additional uncertainty. The uncertainty of this type can be determined on the basis of calibration certificate. It is considered that the probability density function for this type of uncertainty is of Gaussian type.

Uncertainty of the anisotropy - u(A)

Anisotropy is defined as the maximum deviation from the geometric mean of maximum and minimum value when the sensor is rotated around the ortho-axis (e.g., probe handle, rigid or flexible feed-line assembly, "virtual handle"). Anisotropy can be determined using the following expression:

$$A = 20 \cdot \log_{10} \left(\frac{S_{\text{max}}}{\sqrt{S_{\text{max}} \cdot S_{\text{min}}}} \right) dB$$
(4)

where S is the measured amplitude in the field strength units.

The probability distribution is considered to be rectangular. The uncertainty of the anisotropy should be taken into account when triaxal (isotropic) probe is used. Instead, when monoaxial probe is used the Uncertainty caused by the usage of monoaxial probe should be used (explained in the following text).

Uncertainty caused by the usage of monoaxial probe - u(MA)

When monoaxial probe is used, additional correction factor should be apllied (i.e., to be added to the measurement readings). In addition consequently the usage of monoaxial probe causes additional unncertainty in measurement readings and should be taken into account.

Due to the complex mechanisms of radio wave propagation, this type of uncertainty is hard to analyze theoretically (or by simulations) and can be determined by measuring in the field.



Uncertainty caused by mismatching - u(VSWR)

When two elements of the radio equipment are connected to each other, the impedance mismatching occurs to some extent. Due to this effect, a separate component of uncertainty is introduced. The upper limit of the uncertainty caused by mismatching can be determined as follows:

$$u(VSWR) = 100 \cdot \Gamma_e \Gamma_a \quad \%$$
 (5)

where Γ_e denotes reflection coefficient of measuring device and Γ_a denotes the reflection coefficient of the antenna at the antenna feeding-point.

The exact values of VSWR factors (which are generally complex) are usually not known for the individual frequency components, but using the worst-case principle the value of VSWR determined for the entire frequency range can be used. This approach will be applied as well for calculating the combined uncertainty. Of course, in this way, generally, the higher values of uncertainty Γ_a are obtained than it is actually the case. It is considered that the corresponding probability distribution function is of U type.

Uncertainty caused by "electrical noise" - u(Noise)

Electrical noise is the signal detected by the measurement system even if the transmitters of the analyzed systems are not transmitting. The sources of these signals include RF noise (lighting systems, the scanning system, grounding of the laboratory power supply, etc.), electrostatic effects (movement of the probe, people walking, etc.) and other effects (light detecting effects, temperature, etc.). The electrical noise level shall be determined by three different coarse scans in the unused parts of the observed frequency range (essentially, the scans should be carried out with RF sources/transmitters switched off, what, of course, is impossible). None of the evaluated points shall exceed –30 dB of the highest incident field being measured. Within this constraint, the uncertainty due to noise shall be neglected.

Uncertainty caused by drift in the transmitting powers, measurement equipment, temperature and humidity - u(Drift)

The drift due to electronics of the transmitters and the measurement equipment, as well as temperature and humidity, are controlled by the first and last step of the measurement process defined in the measurement procedure and the resulting error should be less than \pm 5 % [30]. The uncertainty shall be evaluated assuming a rectangular probability distribution.

At this point, several important facts should be emphasized:

• uncertainty stemming from temperature variations of measuring equipment is taken into consideration through a separate factor of uncertainty (discussed within the uncertainty caused by measurement devices),



- according to the manufacturer's specification uncertainty stemming from the humidity can be ignored (if the prescribed operating conditions are observed),
- the sources of electromagnetic radiation belonging to the modern professional radio systems (GSM/UMTS/LTE base stations, TV and FM radio transmitters, etc.). Typically work under controlled environmental conditions (use of air conditioners, dehydrators, ...). The uncertainty which is caused by instability of base station transmitters is typically less than 2%. In all other cases, the value of 5% should be used as stipulated in the standard [28].

Uncertainty caused by human bodies - u(Body)

The presence of the human bodies during the measurements affects the measured results. However, when dosimeter is used at stationary positions (for example, lampposts), in all cases the minimum distance between the measurement probe and the bodies of the humans as well as any reflecting object shall be far enough so that the influence of the human bodies can be neglected. In all other cases uncertainty caused by human bodies [30] should be taken into consideration.

Uncertainty caused by small-scale fading - u(Fad)

In a wireless system, the characteristic that transmitted signal loses its deterministic properties and becomes incidental in time and space domain is described with the notion of fading. Essentially, the received signal is affected by both long-term (large-scale) fading and short-term (small-scale) fading. The long-term fading corresponds to the locally averaged electric field strength and is mainly caused by the environment profile between the transmitter and the receiver. On the other hand, the short-term fading is mainly caused by multi-path reflections. In practice, it is impossible to anticipate short-term signal fluctuations only on the basis of physical rules of signal propagation. Actually, it is only possible to talk about statistical characteristics of received electric field strength. According to the standard [30], to assess human exposure to electromagnetic fields, it is recommended to conduct multiple tests (on line or surface defined positions), and perform spatial averaging.

Uncertainty caused by small-scale fading (and which is dependent on the spatial averaging) can be determined based on the [30].

Uncertainty caused by telecommunication traffic and transmitter functionalities - u(Traff)

Besides the well-known short-term fading, which generally characterizes propagation of radio waves, several additional effects have also significant influence on the EMF strength in the mobile networks environment. The most important effects are [27]: traffic load, automatic transmitter power control and discontinuous transmission (section 4.2).

The total BS Tx power directly depends on the number and throughputs of the active connections, i.e. its traffic load. In the case of GSM/DCS systems, depending



on the traffic load, transmitters are turned on or off. On the other side, in the UMTS and LTE system, the increase in the traffic load forces transmitters to operate at higher power and vice-versa.

BS traffic load varies during the day and depends on: the applied tariff profiles, the time of the day, the day of the week, the location of BS... As a rule, mobile operator configures the BS in such a way that under certain conditions it satisfies the traffic demands in the so-called busy hour (the sliding 60-minutes period during which the maximum total traffic load occurs in a given 24-hours period). It should be noted that even if the BS is operating with maximum traffic load, the number of active traffic channels is not constant because of the stochastic nature of call arrivals and call durations.

For each individual connection, the BS Tx power is automatically adjusted depending on the propagation conditions in which the mobile terminal resides. Automatic power control is implemented with a frequency of about 2 Hz in GSM/DCS system, with 1500 Hz in UMTS.

During an established call, when the user makes a normal pause in speech, the base station temporarily stops transmission (in GSM/DCS system transmitters are turned off, while the traffic channel is not transmitted in the UMTS and LTE systems) [28]. Typically, due to this functionality, for each voice connection, the BS transmitters are inactive approximately 40-50% of time.

All the previously mentioned effects lead to greater instability of the DL EMF strength at the measurement position. For this reason, an additional uncertainty stemming from telecommunications traffic must be taken into account. The value of the uncertainty of this type is determined on the basis of daily traffic profiles obtained by measurements.

Total (combined) standard uncertainty

The uncertainty caused by the measurement system (data derived from calibration certificates and technical specifications), can be in principle determined in two ways:

- Adopting appropriate uncertainity values for the examined range of measured values (eg, considering only the data from the frequency range to be tested, the actual value of temperature, etc.). In this way the lower value for the total measurement uncertainty is obtained. However, determining the specific values of individual uncertainties caused by the measurement system is required for each test.
- Adopting the uncertainty values for the broader (or whole) range of the measuring device. In this way, the higher value for the total measurement uncertainty is obtained. However, determining the values of individual uncertainties caused by measurement system is carried out only once.

In practice, the second method is more often used.

Starting from the assumption that the individual uncertainties are mutually uncorrelated, the combined uncertainty shall then be evaluated according to the following equation:



$$u_{c} = \sqrt{\sum_{i=1}^{m} c_{i}^{2} \cdot u_{i}^{2}}$$
 (6)

where c_i is the weighting coefficient (sensitivity coefficient - usually equals 1).

Expanded uncertainty

As recommended by the standards, the expanded uncertainty shall be evaluated using a confidence interval of 95 % [26]. Formally, the expanded uncertainty is obtained by multiplying the total standard uncertainty with factor of k = 1.96.

EXAMPLE 1: Evaluation of measurement uncertainty when LEXNET dosimeter is at a fixed position (triaxial sensor)

cause of uncertainty	reference	specified uncertainty [%]	ncertainty pdf		Standard uncertainty
measuring device	datasheet	18.85	rectangle	1.73	10.90
calibration of the sensor	calibration certificate	23.00	normal (k=2)	2.00	11.50
antenna factor interpolation	calibration certificate	2.20	normal (k=2)	2.00	1.10
anisotropy	datasheet	27.00	rectangle	1.73	15.61
mismatching	datasheet	6.70 $(\Gamma_e$ =0.2, Γ_a =0.33 $(VSWR$ =2))	U- function	1.41	4.75

Combined standard uncertainty of measuring system [%]: 22.77

Expanding Factor: 1.96

Expanded uncertainty of measuring system [%]: 44.62

instability of transmitters	datasheet	2.00	rectangle	1.73	1.16
Telecommunication traffic	measurements	7.40	normal (k=1)	1.00	7.40
small-scale fading	standard	14.0	normal (k=1)	1.00	14.0

Combined standard measurement uncertainty of [%]: 27.76

Expanding Factor: 1.96

Expanded measurement uncertainty [%]: 54.40

Version: V2.0



EXAMPLE 2: Evaluation of measurement uncertainty when LEXNET dosimeter is at a fixed position (monoaxial sensor)

cause of uncertainty	reference	specified uncertainty [%]	pdf	Scaling factor	Standard uncertainty
measuring device	datasheet	18.85	rectangle	1.73	10.90
calibration of the sensor	calibration certificate	23.00	normal (k=2)	2.00	11.50
antenna factor interpolation	calibration certificate	2.20	normal (k=2)	2.00	1.10
monoaxial probe	literature	34.00	normal (k=2)	2.00	17.00
mismatching	datasheet	6.70 $(\Gamma_e$ =0.2, Γ_a =0.33 $(VSWR$ =2))	U-function	1.41	4.75

Combined standard uncertainty of measuring system [%]: 23.74

Expanding Factor: 1.96

Expanded uncertainty of measuring system [%]: 46.54

instability of transmitters	datasheet	2.00	rectangle	1.73	1.16
Traffic load	system characteristics	7.40	normal (k=1)	1.00	7.40
small-scale fading	standard	14.00	normal (k=1)	1.00	14.00

Combined standard measurement uncertainty of [%]: 28.56

Expanding Factor: 1.96

Expanded measurement uncertainty [%]: 55.98

Version: V2.0

FP7 Contract n°318273



APPENDIX 4: PRESENTATION OF THE CHANNEL MODEL USED IN SECTION 4

The models used in section 4 are simplified versions of WINNER2/WINNER+ based models.

 The number of paths strongly depends on the environment and LOS or NLOS configuration. Its statistics is ("roughly") normally distributed with a lower threshold of one and as it is an integer, precisely:

$$N = \max \left[1, \left\lfloor N \left(\mu_N, \sigma_N \right) \right\rfloor \right] \tag{7}$$

where $\mu_N(Env) = E[N]$, $\sigma_N(Env)$ is the standard deviation, all depending on the environment, N the normal distribution and $|\cdot|$ the integer part.

• The MPCs arrival azimuth angles are normally distributed (and wrapped, modulo $[2\pi]$), i.e. :

$$\varphi_n = N \ (\Phi, \sigma_{\varphi}) [360^{\circ}] \tag{8}$$

where Φ is uniformly distributed over [0, 2π [(as the sensor orientation is random), and the RMS Azimuth Spread at Arrival (ASA) is also normally distributed, lower bounded by 1°, i.e., in [°]:

$$\sigma_{\varphi} = \max[1, N \ (\mu_{ASA}, \sigma_{ASA})] \tag{9}$$

where $\mu_{ASA}(Env) = \mathbb{E}\left[\sigma_{\varphi}\right]$, $\sigma_{ASA}\left(Env\right)$ is the spread standard deviation, all depending on the environment.

The LOS path (Environments 2 or 4) is treated specifically. Its DoA (Direction of Arrival) is taken to be the closest one to the mean angle Φ of the distribution, and its power relative to the power sum of the other paths is considered to be given by the Ricean K-factor. This K-factor is generated by assuming it is lognormally distributed, with mean and variance given in Table 22 (of D3.2 main document).

• The MPC arrival elevation angles are (truncated) Laplacian distributed, i.e., in [°]:

$$\theta_n = L\left(\mu_{\theta}, \sigma_{\theta}\right) \tag{10}$$

where $\mu_{\theta}(Env) = E[\theta_n]$, and the RMS Elevation Spread at Arrival (ESA) is lognormally distributed, lower bounded by 1°, i.e., in [°]:

$$\sigma_{\theta} = \max[1, LN \ (\mu_{ESA}, \sigma_{ESA})] \tag{11}$$

where $\mu_{ESA}(Env) = \mathbb{E}[\sigma_{\theta}]$, $\sigma_{ESA}(Env)$ is the spread standard deviation, all depending on the environment.

The elevation statistics, not used in this section, will be used in the following.

The vertical polarization path (field) amplitudes are Rayleigh distributed (NLOS scenarios), i.e.:

FP7 Contract n°318273



$$\left| E_{i0,n}^{V} \right| = R\left(\sigma_{n} \right) \tag{12}$$

where the variance of the Rayleigh distribution is a Laplacian function depending on the path azimuth:

$$\sigma_n^2 = \kappa \exp\left(-\sqrt{2}\left|\varphi_n - \Phi\right| / \sigma_\varphi\right) \tag{13}$$

Note that, for simplicity reasons, and because the amplitude statistics with respect to the elevation are not very well known (there is a lack of information in the literature regarding this point) the power spread does not depend here on the elevation spread.

 The horizontal polarization path amplitudes are derived from the vertical ones through the XPR; i.e.:

$$\left| E_{i0,n}^H \right|^2 = x p r_n^{-1} \left| E_{i0,n}^V \right|^2 \tag{14}$$

where the XPR is lognormally distributed, i.e.:

$$xpr = LN \ (\mu_{XPR}, \sigma_{XPR}) \tag{15}$$

with the mean and standard deviation, indicated in Table 22 (of D3.2 main document) for the considered environments, are expressed in dB (i.e. $xpr = 10^{XPR/10}$),

and the κ constant is obtained through the normalization relation:

$$\sum_{n=1}^{N} \left| E_{i0,n}^{V} \right|^{2} (1 + xpr_{n}^{-1}) = 1$$
(16)

which means that the total field amplitude is always set to 1 V/m.

• To conclude, for LOS scenarios, the total amplitude statistics are Ricean distributed. The LOS path (Environments 2 or 4) is treated specifically. Its DoA is taken to be the closest one to the mean angle Φ of the distribution, and its power relative to the power sum of the other paths is considered to be given by the Ricean K-factor. This K-factor is generated by assuming it is lognormally distributed, with mean and variance given in Table 22 (of D3.2 main document), and Table 6. Following the renormalization of the path powers, the azimuth spread is not recomputed.



Table 6 : Parameters WINNER2/WINNER+ channel models for ten environments.

Env. n°	Local environment	Visibility from BS/AP	WINNER scenario	K factor Mean / Std (dB)	XPR Mean/Std (dB)	Azimuth Spread Mean/Std (°)	Elevation Spread Mean/Std (°)	Nb clusters Mean/Std
1	Indoor small office / residential	NLOS	A1/NLOS	-	10/4	49/7	13/1.5 1.6/1.10/0.17	16/4.5
2	Indoor small office / residential	LOS	A1/LOS	7/6	11/4	45/9	9/2 1.6/.94/0.26	12/6
3	Typical Urban (Hot spot)	NLOS	B1 (UMi)	_	8/3	35.5/35	2/0.88/0.16	16/3
4	Typical Urban (Hot spot)	LOS	B1 (UMi)	9/6	9/3	25/28.5	2/0.6/0.16	8/3.5
5	Metropolitan suburban	NLOS	C1 (SMa)	_	7/3	44.5/20	7/1.00/0.16	14/3
6	Metropolitan suburban	LOS	C1 (SMa)	9/7	8/4	30/8	5.5/1.08/0.16	15/3.5
7	Metropolitan O2I	NLOS	A2, B4, C4	_	9/11	18/13	10/8 1.2/1.01/0.43	12/2.5
8	Indoor (Hot spot)	LOS	В3	2/3	9/4	38/8.5	A1 LOS	10/6
9	Typical UMa	NLOS	C2	_	7/3	52.5/20.5	9/10 10/1.26/0.16	20/4
10	Typical UMa	LOS	C2	7/3	8/4	50/18.5	18/10 6/0.95/0.16	8/3



APPENDIX 5: DETAILS AND MEASUREMENTS OF THE EXTRAPOLATION FROM MONOAXIAL TO ISOTROPIC FIELD PROBE STUDY

Unlike in section 4 of main D3.2 document (body-worn configuration), the current study considers the dosimeter isolated based on measurement results.

Having in mind that the propagation and depolarization of EM waves depend on the environment, measurements were conducted in seven different scenarios.

Measurement results of electric field strength for all three spatial components E_X , E_Y and E_Z , and total electric field strength $^{E_{tot}}$ are presented in Figure 21, for scenario 1 as an example. Accompanying extrapolation factors n_X , n_Y , n_Z and n_Z are shown in Figure 22 while the corresponding statistical values are given in Table 7. Probability density function for factor n_Z are shown in Figure 23. For comparison of all seven scenarios uncertainties for extrapolation factors n_X , n_Y , n_Z and n_Z are shown in Table 7. Using these values, mean values for $^{n_{Qverail}}$ are determined. For all other scenarios, the measurement results have similar behaviour.

Scenario 1 is representing indoor propagation environment with both LOS and NLOS conditions. In scenario 1, measurements were performed in an urban area and in indoor environment. Transmitting antennas of the nearest base stations were installed indoor. The route of measurement system comprised the measurement points in which LOS (visibility with at least one of transmitting antennas) and NLOS conditions were approximately equally represented.

Propagation environment with indoor receiving area and outdoor transmitting antennas is represented in scenario 2. For scenario 2, measurements were performed in an urban area and in indoor environment. Transmitting antennas of the nearest base stations were not installed indoor.

In scenario 3, measurements were performed in urban area and in outdoor environment. Transmitting antennas of the nearest base stations were installed outdoor. The route of measurement system comprised the measurement points where LOS conditions with at least one of base station antennas were satisfied.

Scenario 4 represents the underground railway station. In this scenario measurements were performed in the station platform. The nearest base stations were installed indoor in underground railway station. Most of the measurement points had LOS conditions with at least one of base station antennas.

In scenario 5, measurements were performed in dense urban area and in pedestrian area outdoor environment. Transmitting antennas of the nearest base stations were installed outdoor. The route of measurement system comprised the measurement points where LOS conditions with at least one of base station antennas were satisfied.

Version: V2.0 31



Scenario 6 is representing suburban outdoor propagation environment with both LOS and NLOS conditions. Transmitting antennas of the nearest base stations were installed outdoor. The route of measurement system comprised the measurement points with LOS conditions (approximately 75%) and NLOS conditions (approximately 25%).

In scenario 7, measurements were performed in rural area and in outdoor environment. Transmitting antennas of the nearest base stations were installed outdoor. The route of measurement system comprised the measurement points where LOS conditions were satisfied.

These seven scenarios are representing environments where most of population is exposed. On the other hand, these environments are representing seven different environments with regards to propagation and depolarization of radio-frequency electromagnetic waves. Thus the figures 21 to 23 and tables 7 and 8, present the detailed results of extrapolation factors statistics.

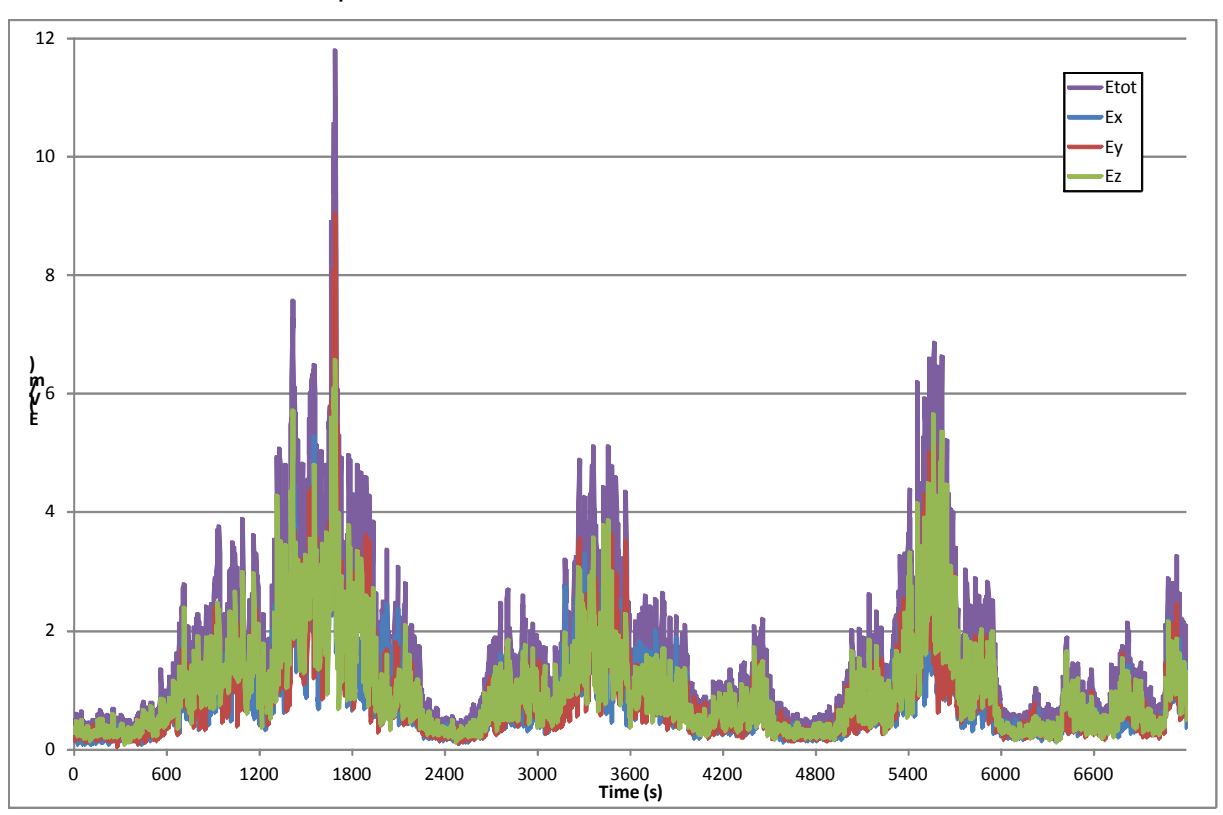


Figure 21 Electric field strength (mV/m) with regards to time for scenario 1

Version: V2.0



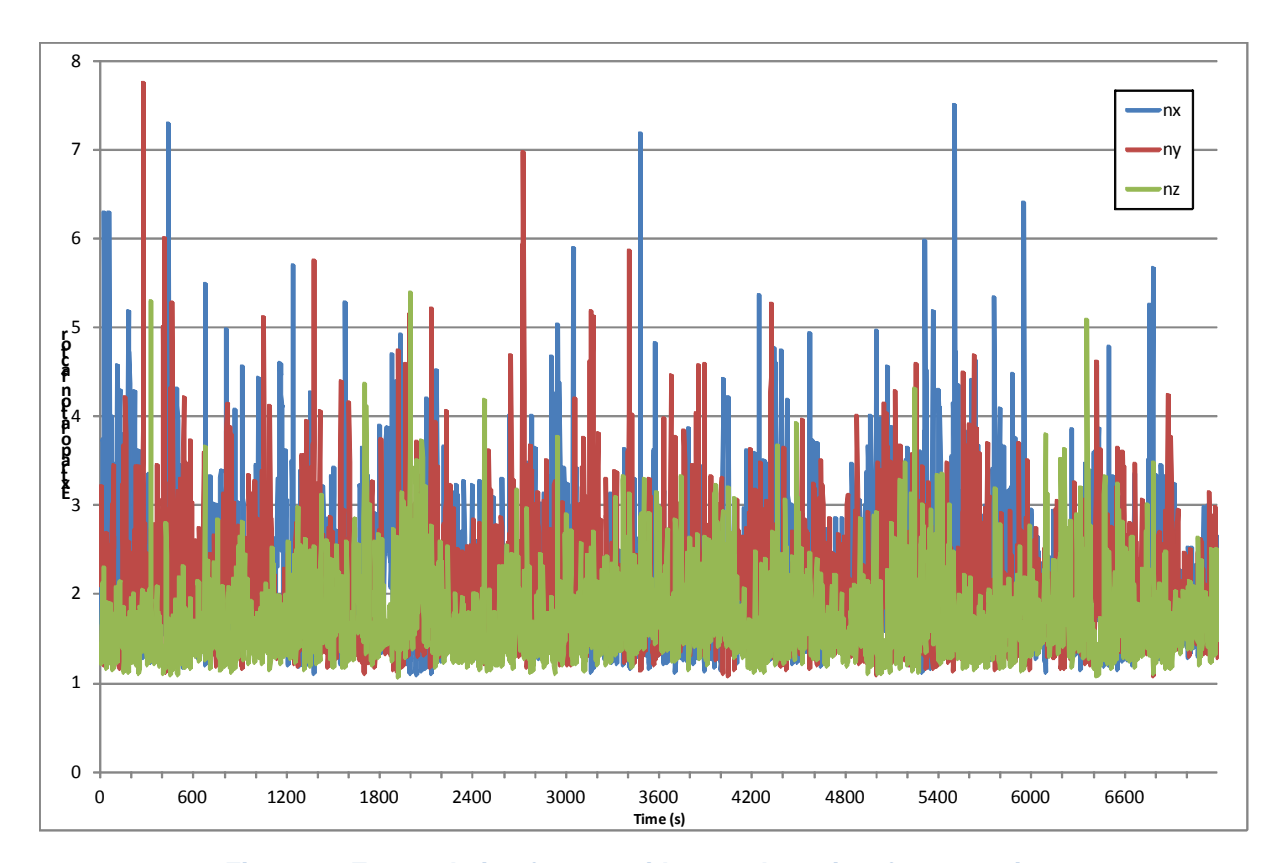


Figure 22 Extrapolation factors with regards to time for scenario 1

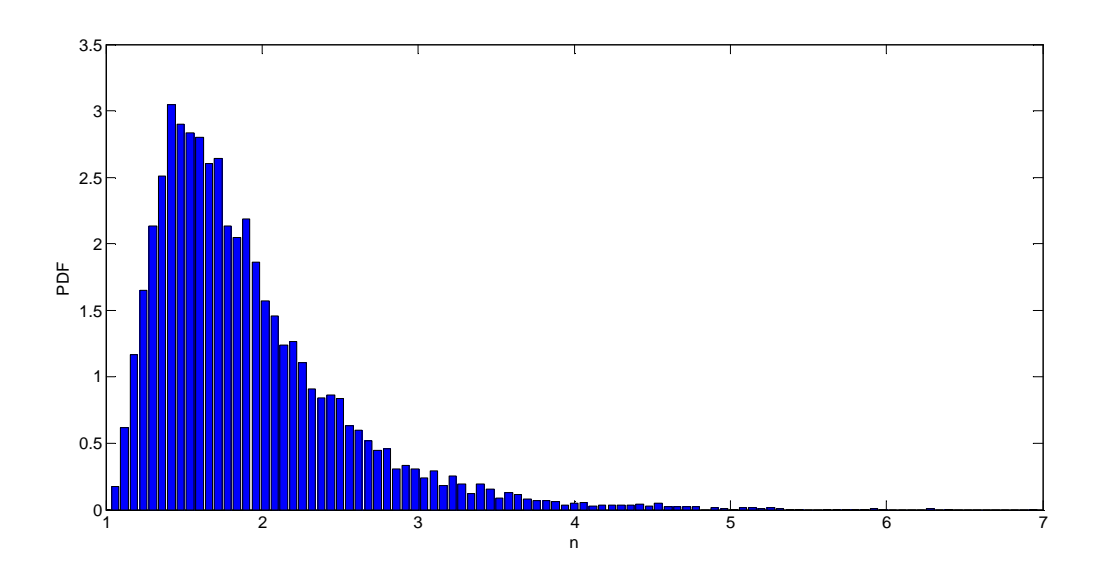


Figure 23 Probability density function for extrapolation factor n for scenario 1



Table 7: Mean values, medians, standard deviations and uncertainties of extrapolation factors

Scenario	Statistical parameter	n_X	n_{Y}	n_Z	n
	Mean	2.08	2.03	1.70	1.94
Scenario 1	Median	1.91	1.89	1.60	1.78
	Standard deviation	0.71	0.65	0.44	0.63
	Uncertainty (%)	33.99	31.94	25.78	32.61
	Mean	2.10	1.87	1.65	1.87
Scenario 2	Median	2.02	1.76	1.59	1.76
	Standard deviation	0.56	0.43	0.31	0.48
	Uncertainty (%)	26.75	23.17	18.71	25.86
	Mean	2.00	1.89	1.76	1.88
Scenario 3	Median	1.90	1.78	1.67	1.77
	Standard deviation	0.58	0.49	0.45	0.52
	Uncertainty (%)	28.81	26.22	25.33	27.49
Scenario 4	Mean	1.96	2.32	2.01	2.10
	Median	1.74	2.00	1.72	1.83
	Standard deviation	0.85	1.00	0.92	0.94
	Uncertainty (%)	43.26	43.25	45.67	44.77
	Mean	2.20	2.30	1.56	2.02
Scenario 5	Median	1.99	2.06	1.49	1.79
	Standard deviation	0.84	0.87	0.32	0.79
	Uncertainty (%)	38.18	37.62	20.79	39.20
	Mean	2.00	1.89	1.64	1.84
Scenario 6	Median	1.94	1.86	1.56	1.78
Scenario 6	Standard deviation	0.41	0.36	0.35	0.40
	Uncertainty (%)	20.59	18.88	21.19	21.83
	Mean	2.07	1.81	2.15	2.01
Scenario 7	Median	1.77	1.53	2.00	1.79
Scenario 7	Standard deviation	0.94	0.74	0.65	0.80
	Uncertainty (%)	45.36	40.84	30.07	39.70

Table 8 Comparison of mean values, medians, standard deviations and uncertainties for n for all scenarios

Scenario	1	2	3	4	5	6	7	Overall
Mean	1.94	1.87	1.88	2.10	2.02	1.84	2.01	1.95
Median	1.78	1.76	1.77	1.83	1.79	1.78	1.79	1.79
Standard deviation	0.63	0.48	0.52	0.94	0.79	0.40	0.80	0.65
Uncertainty (%)	32.61	25.86	27.49	44.77	39.20	21.83	39.70	33.07



APPENDIX 6: SPECTRUM RESULTS FOR THE DOSIMETER STUDY IN REAL ENVIRONMENT

This appendix 6 presents details related to the section 4.4.2 of D3.2 document.

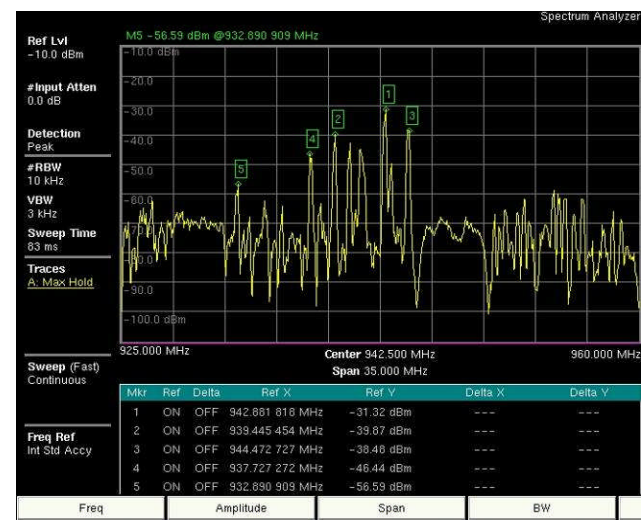
Spectrum analyser measurements have been done using the max-hold function of the spectrum analyser and a screen capture has been obtained after few seconds in order to see all the operators present at a given location. Markers have been placed at important values marking the different bands.

Continuous

| Continuous | Continuous | Continuous | Continuous | Continuous | Continuous | Continuous | Continuous | Continuous | Continuous | Continuous | Continuous | Continuous | Continuous | Continuous | Continuous | Continuous | Continuous | Continuous | Continuous | Continuous | Continuous | Continuous | Continuous | Continuous | Continuous | Continuous | Continuous | Continuous | Continuous | Continuous | Continuous | Continuous | Continuous | Continuous | Continuous | Continuous | Continuous | Continuous | Continuous | Continuous | Continuous | Continuous | Continuous | Continuous | Continuous | Continuous | Continuous | Continuous | Continuous | Continuous | Continuous | Continuous | Continuous | Continuous | Continuous | Continuous | Continuous | Continuous | Continuous | Continuous | Continuous | Continuous | Continuous | Continuous | Continuous | Continuous | Continuous | Continuous | Continuous | Continuous | Continuous | Continuous | Continuous | Continuous | Continuous | Continuous | Continuous | Continuous | Continuous | Continuous | Continuous | Continuous | Continuous | Continuous | Continuous | Continuous | Continuous | Continuous | Continuous | Continuous | Continuous | Continuous | Continuous | Continuous | Continuous | Continuous | Continuous | Continuous | Continuous | Continuous | Continuous | Continuous | Continuous | Continuous | Continuous | Continuous | Continuous | Continuous | Continuous | Continuous | Continuous | Continuous | Continuous | Continuous | Continuous | Continuous | Continuous | Continuous | Continuous | Continuous | Continuous | Continuous | Continuous | Continuous | Continuous | Continuous | Continuous | Continuous | Continuous | Continuous | Continuous | Continuous | Continuous | Continuous | Continuous | Continuous | Continuous | Continuous | Continuous | Continuous | Continuous | Continuous | Continuous | Continuous | Continuous | Continuous | Continuous | Continuous | Continuous | Continuous | Continuous | Continuous | Continuous | Continuous | Continuous | C

(a) Location#1

(b) Location#2



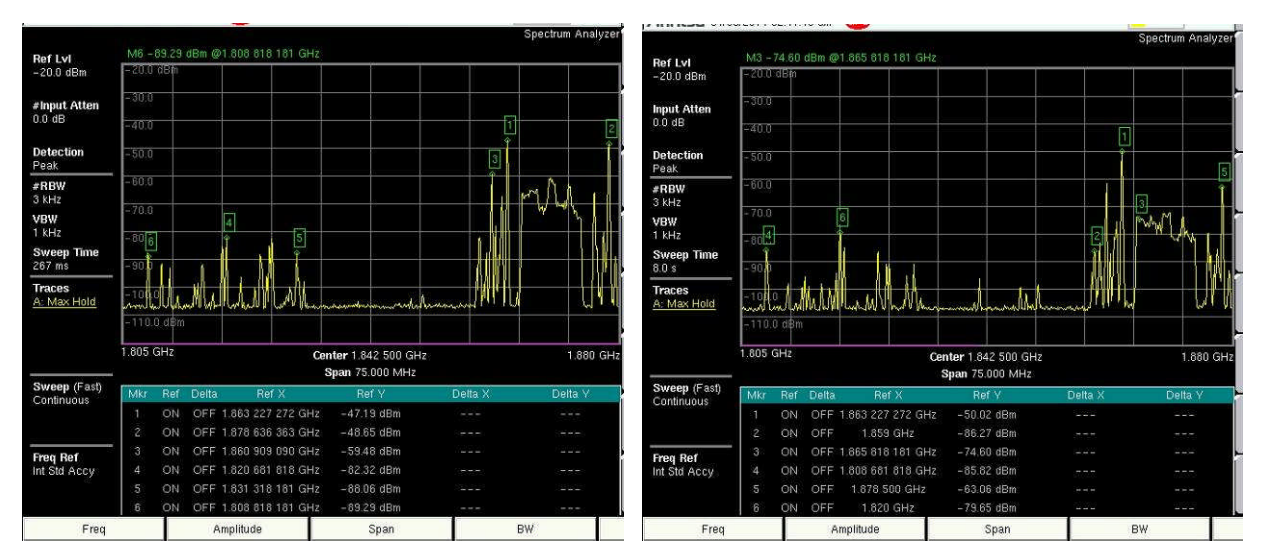
(c) Location#3

Figure 24: Spectrum analyser results GSM-DL at the three locations described in Table 41 and Figure 106 of D3.2

Version: V2.0

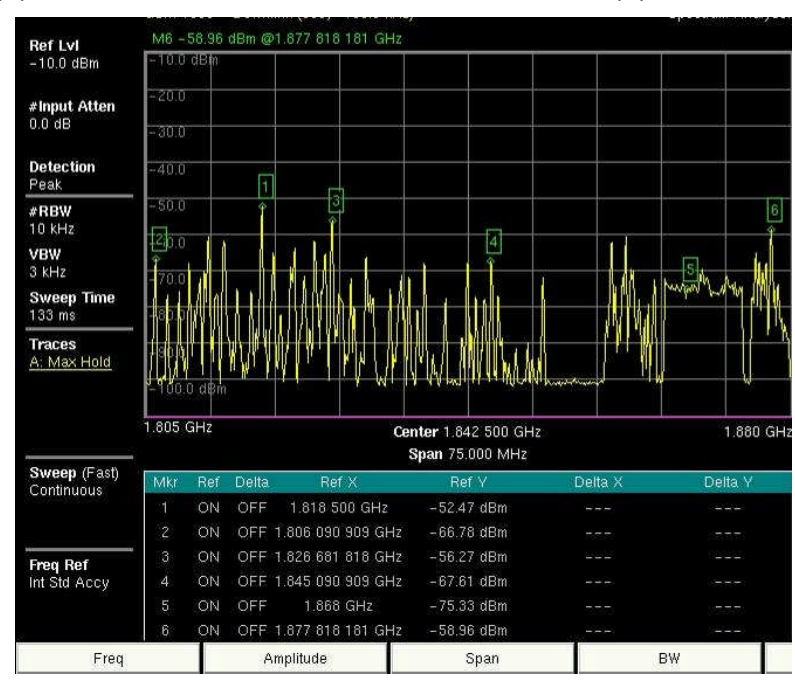


2 DCS-DL band spectrum



(a) Location#1

(b) Location#2



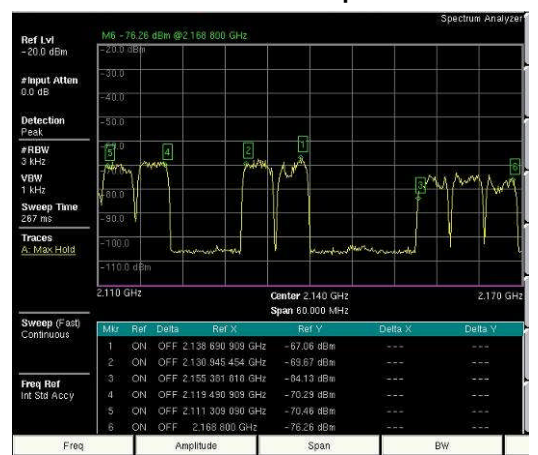
(c) Location#3

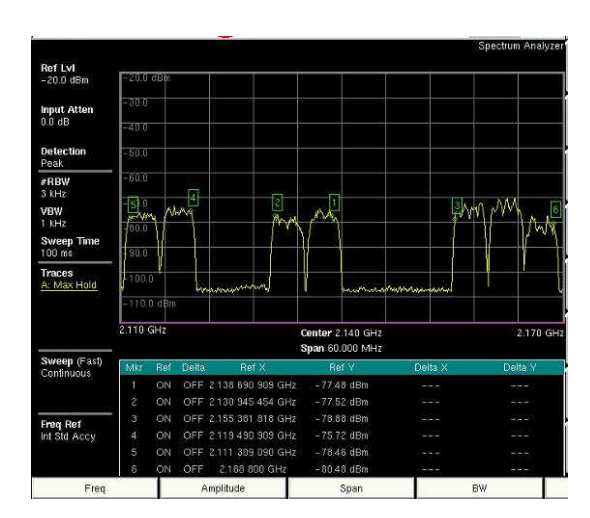
Figure 25: Spectrum analyser results DCS-DL at the three locations described in Table 41 and Figure 106 of D3.2

Version: V2.0



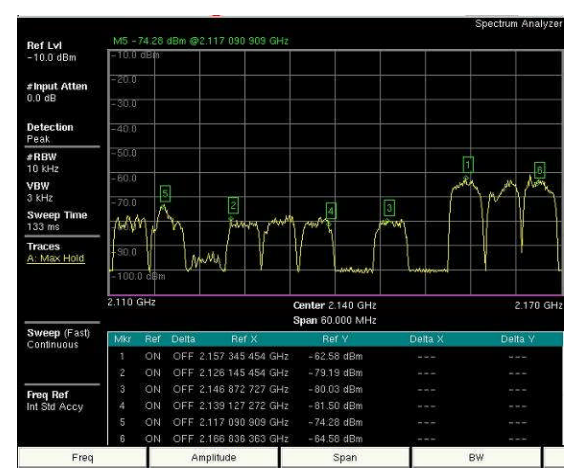
3 UMTS-DL band spectrum





(a) Location#1

(b) Location#2



(c) Location#3

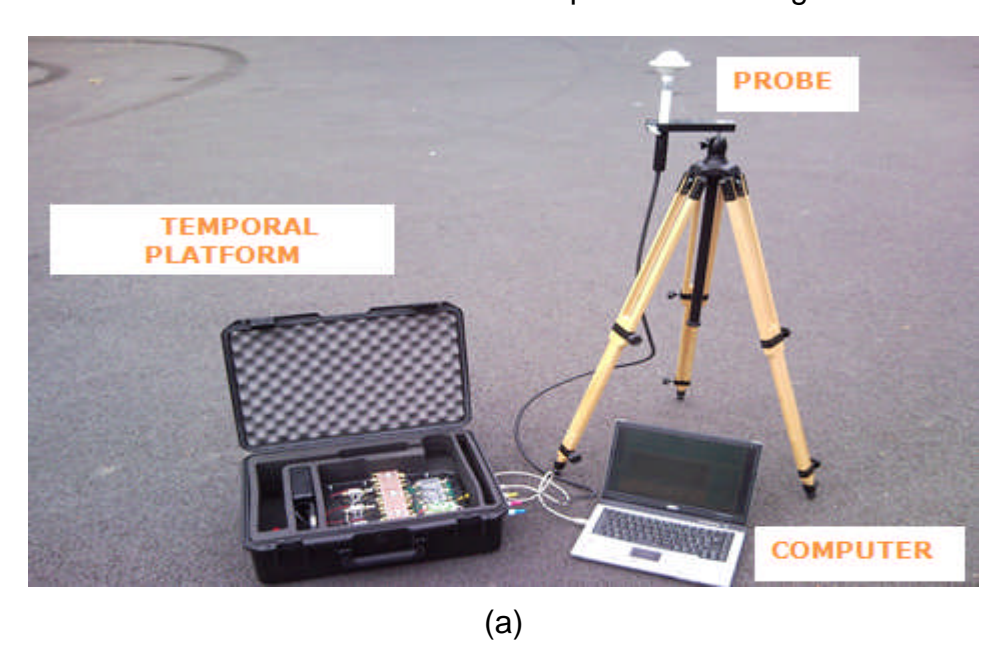
Figure 26: Spectrum analyser results UMTS-DL at the three locations described in Table 41 and Figure 106 of D3.2

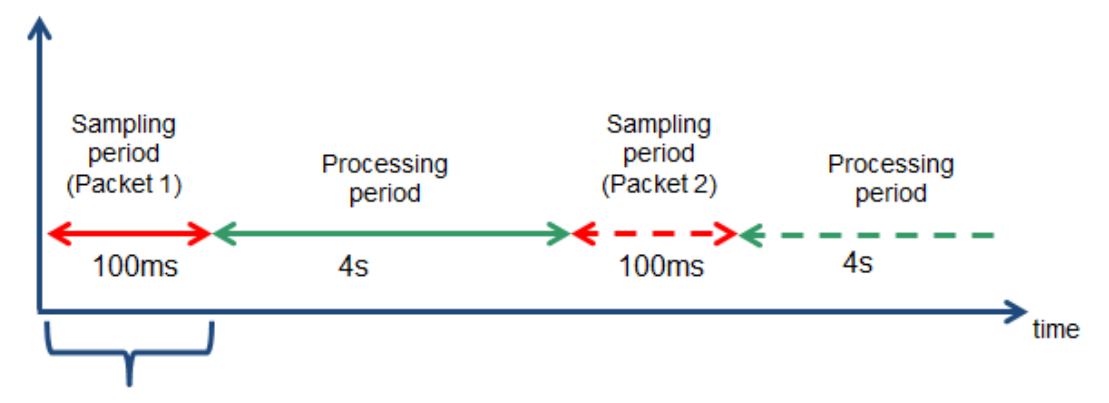
Version: V2.0



APPENDIX 7: STUDY OF OPTIMUM EMF MEASUREMENT METHODOLOGY FOR EXPOSURE EVALUATION

In this section, the study of different signal types and the optimum way to evaluate the EMF exposure level for a particular signal is presented. To achieve this objective, a time-domain based measurement platform was used. This platform can carry out simultaneous EMF measurements on three axis with a sampling period as low as 5 mico-seconds. The measurement setup is shown in Figure 27a.





First acquisition => 14285 samples (sampling period of 7us)

(b)

Figure 27: Time domain based EMF measurement platform (a) measurement setup, (b) measurement technique.

Version: V2.0



The measurement methodology is summarized in Figure 27b. Each measurement period consists of 100 ms during which 14285 samples are acquired per polarization (total of 3 polarizations measured). After that, there is about 4 seconds of post-processing period over which the data is stored in the memory and next measurement cycle is prepared.

Using this platform, four of the most widely used telecommunication signals were measured. Each signal was measured with a sampling rate of 7 microseconds and over a period of 6 minutes. The detailed measurement setup for each standard is summarized in the Table 9. The measurements were carried out over the vertical axis probe only with an RMS power detector. The 6 minutes measurement data was distributed into different number of packages (each package containing 1 frame of the signal) according to the frame length of each signal. Hence, the GSM-DL signal which has a frame length of 4.616 ms would have 660 samples (with a sampling rate of 7us) per package of data, and for each acquisition period of 100 ms of the platform, we will have 21 packages. And thus, over a period of 6 minutes, we will acquire 1890 packages (90 * 21), each with 660 samples corresponding to 1890 frames of GSM-DL signal. The result would be the same for the DCS-DL signal. Similarly we can calculate the number of frames measured for the UMTS-DL and LTE-DL signals.

Frequency bands	Signal frame time	Number of package for one acquisition (100 ms period)	Number of packages for 6 minute measurement period
GSM-DL	4,616ms	21	1890
925 MHz – 960 MHz	(660 samples)		
DCS-DL	4,616ms	21	1890
1805 MHz – 1880 MHz	(660 samples)		
UMTS-DL	6ms	16	1440
2110 MHz – 2170 MHz	(858 samples)		
LTEVII-DL	10ms	9	810
2620 MHz – 2690 MHz	(1429 samples)		

Table 9: Measurement setup for each signal type

The measurements were carried out in the city of Brest, France, at two different locations over a period of three days (Figure 28).

- Location#1 was selected with a direct Line of Sight (LoS) conditions with the Base Station (BS) on a football field with very little variation of the environment (no passage and few buildings around).

Version: V2.0 39



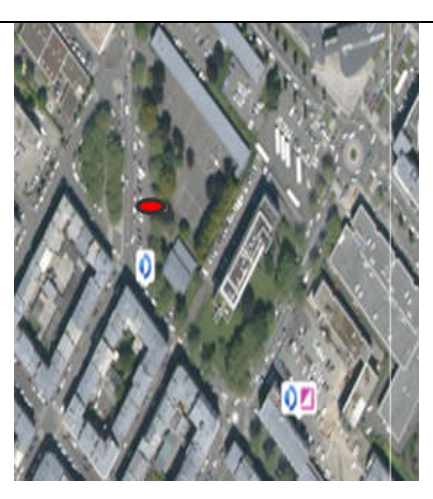
- **Location#2** was in the proximity of large buildings in the city center inside a public car parking space with relatively large variations of environment.





(a) Location#1





(b) Location#2

Figure 28: Locations for the measurements with the time domain based platform.

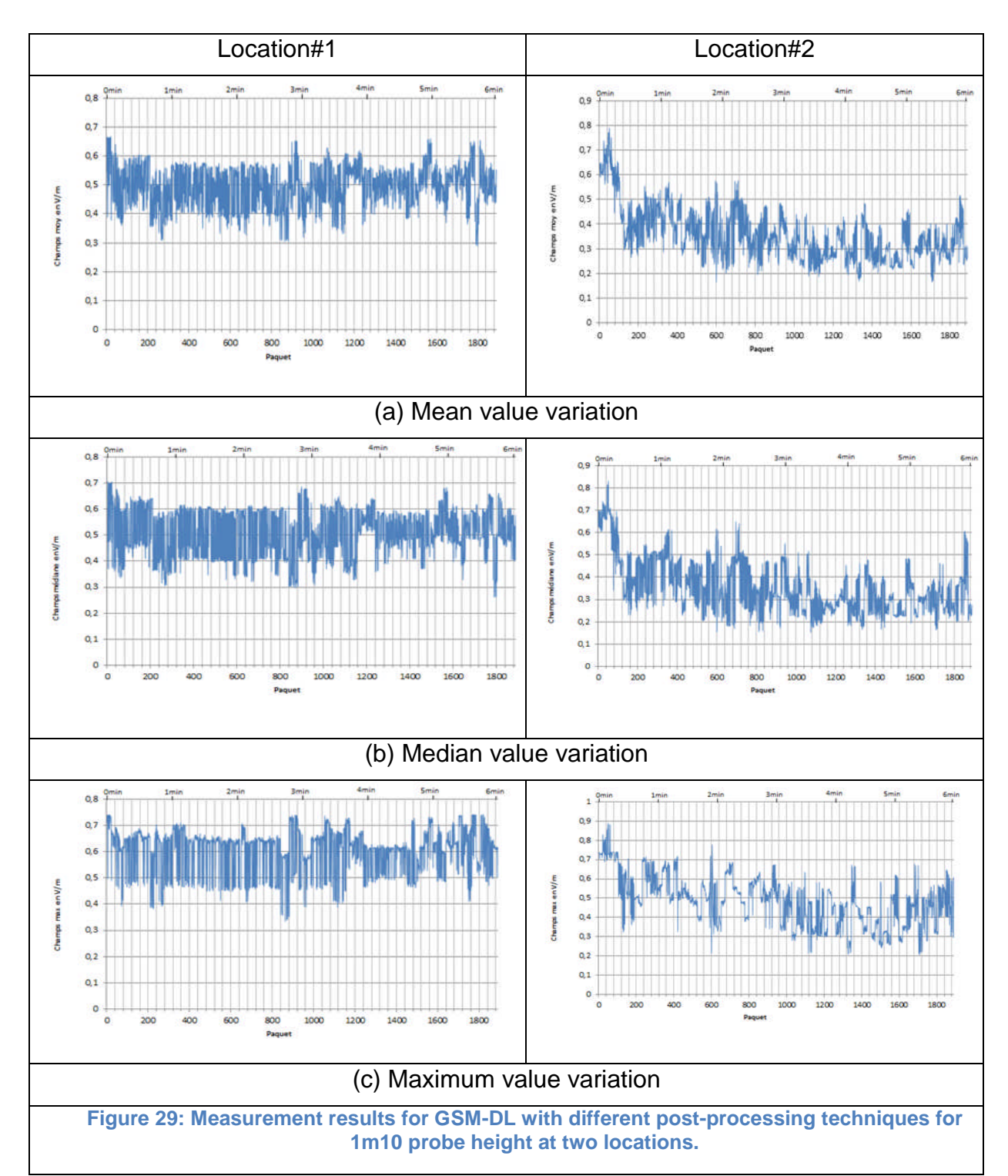
The measurements were carried out with the probe at a heights of 1m10 and 1m70, at each location over a period of 6 minutes each time. The resulting data was post-processed afterwards and the variation of the mean, median, and maximum value (calculated for a single frame) of each signal type was observed over the 6 minutes. Some of the interesting results are presented in the following.

GSM-DL study

Below in Figure 29 details the results of the two locations described in the previous section with the three statistics (mean, median, and maximum) for the GSM-DL frequency band.

Version: V2.0 40





For the location#1, the ANFR (Agence National des Radio Fréquences) carried out measurements which were used as a reference for comparison. According to their report, a 0.61 V/m value was given for the exposure in the 900 MHz frequency band [34]. Similarly for the second location, the ANFR reference value for this band was given at 0.63 V/m according the report [35]. Comparing to the above measurements, we can see a good agreement. It should be noted that the reference

Version: V2.0



values are over-estimated in order to provide the worst case scenario using an extrapolation factor.

Comparing the variation curves over 6 minute measurement cycle for the two locations, we can observe that the E-field is relatively constant at the location#1, due to the direct LoS conditions and a relatively stable environment with few reflections and variations. The measurements from the location#2 are varying significantly as expected due to the varying environment. In order to determine which of the three statistics is the most optimum for the GSM-DL signal, we should base our conclusions on the measurements taken at location #1. Below in Table 10, a quantitative comparison is given between the three calculation methods at location #1. For each calculation approach (mean, median, or maximum), the average value over 6 minutes is calculated, as well as the variation between the maximum and minimum values (in V/m and in dB).

Table 10: Comparison of different techniques for EMF exposure calculation for the GSM-DL signal at location#1

Measurement technique for each frame	Average value over 6 minutes (V/m)		Variation (Max – Min) over 6 minutes (V/m)		Variation (Max – Min) over 6 minutes (dB)	
	1.1m height	1.7m height	1.1m height	1.7m height	1.1m height	1.7m height
Mean value	0.50	0.57	0.33	0.40	± 3.0	± 3.8
Median value	0.51	0.58	0.38	0.44	± 3.3	± 4.0
Maximum value	0.58	0.68	0.40	0.58	± 3.2	± 4.5

Table 11: Comparison of different techniques for EMF exposure calculation for the GSM-DL signal at location#2

Measurement technique for each frame	Average value over 6 minutes (V/m)		Variation (Max – Min) over 6 minutes (V/m)		Variation (Max – Min) over 6 minutes (dB)	
	1.1m height	1.7m height	1.1m height	1.7m height	1.1m height	1.7m height
Mean value	0.36	0.45	0.62	0.47	± 6.8	± 4.9
Median value	0.35	0.45	0.67	0.49	± 7.3	±5.0
Maximum value	0.48	0.62	0.68	0.55	± 6.3	± 4.6

We can see from the Table 10 that the three calculation methods provide similar statistical results. The variation over a 6 minute measurement period is between ±3 dB and ±4.5 dB, which remains in the limits specified by the ANFR report [34] (incertitude of the measured value around 4.6 dB for this location). The statistical data for the second location for the GSM-DL measurement is presented in Table 11

Version: V2.0 42



for comparison. It can be observed that the variation here is larger than measurements at location#1 (as expected).

To conclude the measurement technique study for the GSM-DL signal, the median value method is proposed. It has the advantage of suppressing the GSM-UL signal which is repeated 1/8th of the total GSM frame. The graphical comparison between the measurements at two locations is shown in Figure 30.

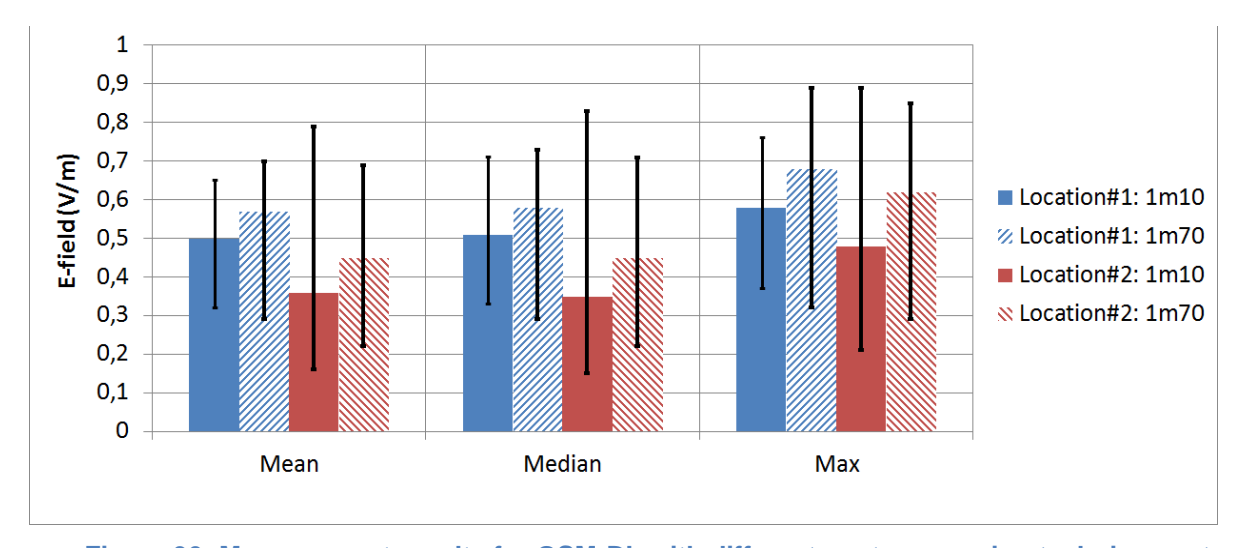


Figure 30: Measurement results for GSM-DL with different post-processing techniques at the two locations.

The results from the above figure show the variation of the average values over 6 minutes calculated using the three proposed calculation methods (mean, median, and max) for a single period, with the maximum and minimum values. We see a similar behavior for the three techniques at the two locations, and for the two different heights. The difference in the average value levels can be attributed to the spatial fading.

DCS-DL study

The temporal variations of the DCS-DL signal over a period of 6 minutes using three different calculations are presented in Figure 30. The statistical data summarizing the measurements at the two locations are presented in

Table 12 and Table 13

Version: V2.0 43



Table 12: Comparison of different techniques for optimum EMF exposure for the DCS-DL signal at location#1

Measurement technique for each	Average value over 6 minutes (V/m)		Variation (Max – Min) over 6 minutes (V/m)		Variation (Max – Min) over 6 minutes (dB)	
frame	1.1m height	1.7m height	1.1m height	1.7m height	1.1m height	1.7m height
Mean value	0,21	0,14	0,14	0,14	±3,1	±3,8
Median value	0,22	0,14	0,16	0,19	± 3,4	± 4,7
Maximum value	0,25	0,22	0,16	0,17	± 2,9	±3,7

Table 13: Comparison of different techniques for optimum EMF exposure for the DCS-DL signal at location#2

Measurement technique for each	Average value over 6 minutes (V/m)		Variation (Max – Min) over 6 minutes (V/m)		Variation (Max – Min) over 6 minutes (dB)	
frame	1.1m height	1.7m height	1.1m height	1.7m height	1.1m height	1.7m height
Mean value	0,20	0,11	0,17	0,12	±4,0	±4,17
Median value	0,20	0,11	0,19	0,16	±4,8	±4,9
Maximum value	0,27	0,16	0,17	0,16	± 2,8	±4,2

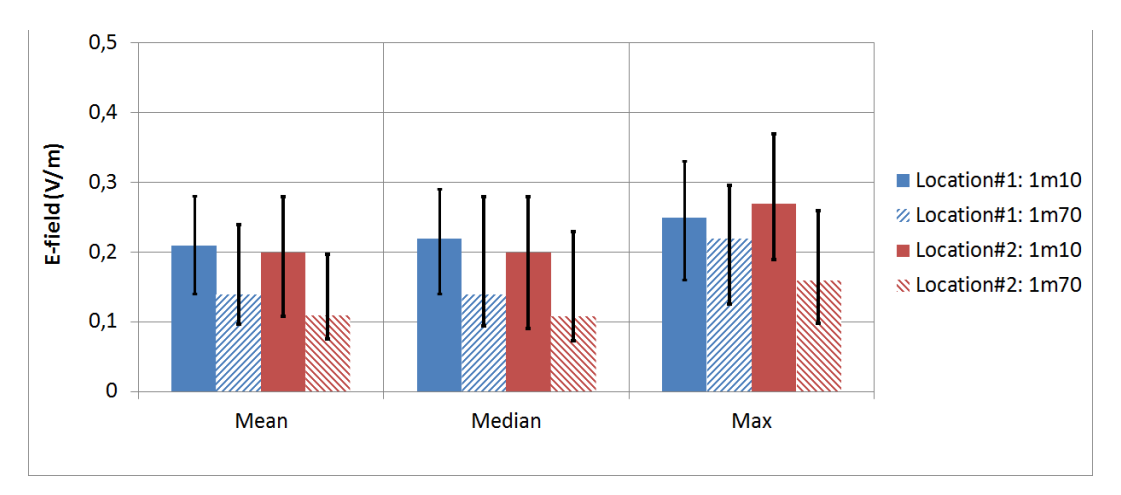


Figure 31: Measurement results for DCS-DL with different post-processing techniques at the two locations.

The graphical representation is shown in Figure 31. It is quite similar to the results for the GSM-DL signal (as both are basically the same). Hence, again the median value calculation method is proposed for the DCS-DL signal. Comparing to

Version: V2.0



the results in the ANFR reports, the E-field value reported in [34] & [35] are around 0.15 V/m (spatial mean over three probe heights) which is in good agreement with our measurements.

UMTS-DL study

For the UMTS-DL study, the statistical date for the two locations is shown in Table 14 and Table 15 below. ANFR reports the E-field values in [34] & [35] at around 0.32 V/m (spatial mean over three probe heights). Again, this is in good agreement with our results.

Table 14: Comparison of different techniques for optimum EMF exposure for the UMTS-DL signal at location#1

Measurement technique for each	Average value over 6 minutes (V/m)		Variation (Max – Min) over 6 minutes (V/m)		Variation (Max – Min) over 6 minutes (dB)	
frame	1.1m height	1.7m height	1.1m height	1.7m height	1.1m height	1.7m height
Mean value	0,52	0,57	0,17	0,76	±1,4	±4,0
Median value	0,58	0,62	0,37	0,72	±2,5	±3,7
Maximum value	0,95	1,00	0,94	0,73	±3,8	±2,8

Table 15: Comparison of different techniques for optimum EMF exposure for the UMTS-DL signal at location#2

Measurement technique for each	Average value over 6 minutes (V/m)		Variation (Max – Min) over 6 minutes (V/m)		Variation (Max – Min) over 6 minutes (dB)	
frame	1.1m height	1.7m height	1.1m height	1.7m height	1.1m height	1.7m height
Mean value	0,23	0,23	0,26	0,17	±4,2	±3,0
Median value	0,24	0,23	0,23	0,18	±3,9	±3,0
Maximum value	0,37	0,34	0,26	0,19	±3,1	±2,4

Version: V2.0



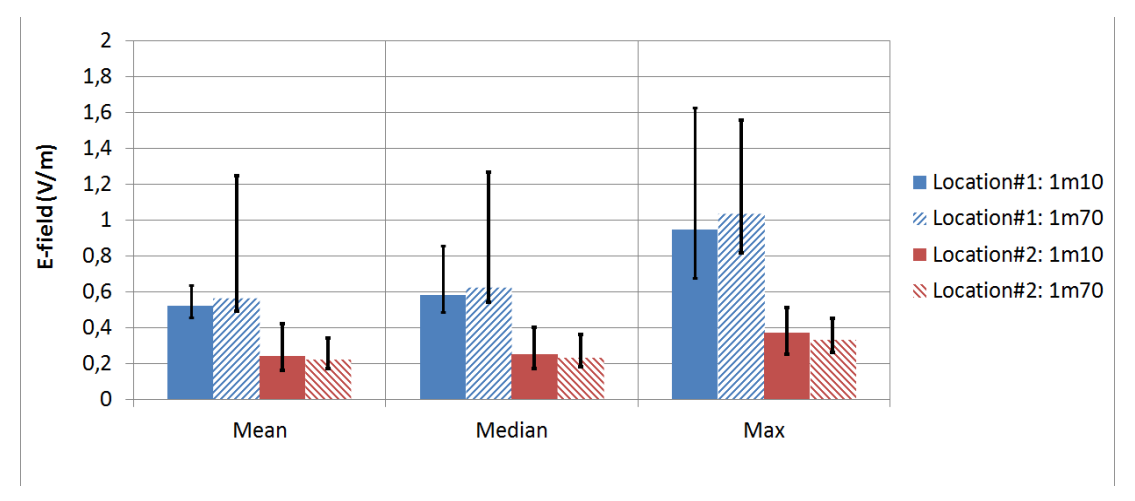


Figure 32: Measurement results for UMTS-DL with different post-processing techniques at the two locations.

The graphical representation of the measurements at the two locations is presented in Figure 32. The strong variation at location#1 for the maximum values is due to few relatively high E-field values which are probably due to passing by people or change in spatial fading.

For the UMTS-DL signal, the mean or the median value calculation method can be adopted as they present similar results.

LTE VII-DL study

Similarly for the LTE VII study, the statistical data is summarized in Table 16 and Table 17 for the two locations respectively. Comparing to the reported values by ANFR at these two locations in [34] & [35], 0.8 V/m are reported at location#1 and lower than 0.05 V/m at location#2. It should be noted that the measurements at location#2 are quite old and since then, the LTE service has been deployed.

Table 16: Comparison of different techniques for optimum EMF exposure for the LTEVII-DL signal at location#1

Measurement technique for each	Average value over 6 minutes (V/m)		Variation (Max – Min) over 6 minutes (V/m)		Variation (Max – Min) over 6 minutes (dB)	
frame	1.1m height	1.7m height	1.1m height	1.7m height	1.1m height	1.7m height
Mean value	0,7	0,23	1,5	0,23	±5,9	±3,4
Median value	0,35	0,14	2	0,32	±12,2	±6,4
Maximum value	1,6	0,64	1,5	0,52	±3,6	±2,9

Version: V2.0 46



Table 17: Comparison of different techniques for optimum EMF exposure for the LTEVII-DL signal at location#2

Measurement technique for each	Average value over 6 minutes (V/m)		Variation (Max – Min) over 6 minutes (V/m)		Variation (Max – Min) over 6 minutes (dB)	
frame	1.1m height	1.7m height	1.1m height	1.7m height	1.1m height	1.7m height
Mean value	0,08	0,07	0,17	0,16	±7,2	±5,9
Median value	0,03	0,05	0,21	0,23	±11,5	±10,3
Maximum value	0,29	0,19	0,38	0,2	±6,5	±4,0

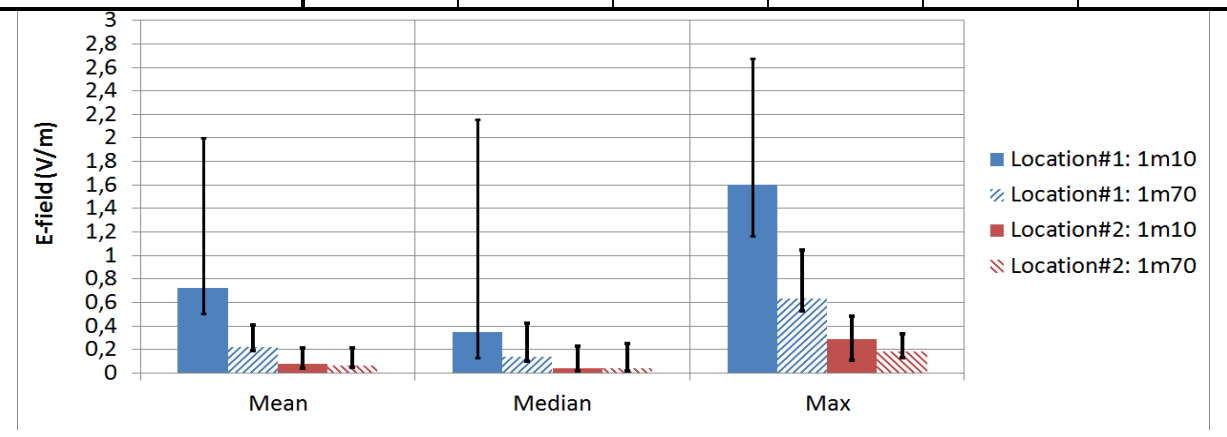


Figure 33: Measurement results for LTE VII-DL with different post-processing techniques at the two locations.

The graphical representation is presented in Figure 33. It can be observed that quite a different behaviour is measured for the location#1 at 1.1 m probe height, with high level of E-field and large values marking a strong variation. These variations are probably due to the change in the environment during the measurements.

To optimally evaluate the LTE-VII DL exposure, the mean value calculation method is proposed. The median method will not be a good choice in this case, as the LTE signal in the time domain is like a pulse with many zero values.

Conclusions

From the above study, the following Table 18 summarizes the proposed calculation methods for each of the four standards.

Version: V2.0 47



Table 18: Proposed measurement techniques for the different telecommunication standards in the down-link scenario.

Frequency standard	Optimum measurement technique
GSM-DL	Median
DCS-DL	Median
UMTS-DL	Median
LTE VII-DL	Mean

References

The references of these appendices can be found in the D3.2 r2 document.

Version: V2.0 48